AD_____

COXIELLA BURNETII VACCINE DEVELOPMENT: LIPOPOLYSACCHARIDE STRUCTURAL ANALYSIS

MIDTERM REPORT

V. N. REINHOLD

DECEMBER 29, 1989

Supported by

U.S. ARMY MEDICAL RESEARCH AND DEVELOPMENT COMMAND
Fort Detrick, Frederick, Maryland 21701-5012

Contract No. DAMD17-88-C-8133

Harvard University School of Public Health
665 Huntington Avenue
Boston, Massachusetts 02115

SECURITY CLASSIFICATION OF THIS PAGE

REPORT DOCUMENTATION PAGE

Form Approved OMB No. 0704-0188

1a. REPORT SECURITY CLASSIFICATION: Unclassified	1b. RESTRICTIVE MARKINGS
2a. SECURITY CLASSIFICATION AUTHORITY	3. DISTRIBUTION/AVAILABILITY OF REPORT: Approved for public release; distribution unlimited
2b. DECLASSIFICATION/DOWNGRADING SCHEDULE	
4. PERFORMING ORGANIZATION REPORT NUMBER(S)	5. MONITORING ORGANIZATION REPORT NUMBER(S)
6a. NAME OF PERFORMING ORGANIZATION: Harvard University School of Public Health; 6b. OFFICE SYMBOL (if applicable)	7a. NAME OF MONITORING ORGANIZATION
6c. ADDRESS (City, State, and ZIP Code): 665 Huntington Avenue, Boston, Massachusetts 02115	7b. ADDRESS (City, State, and ZIP Code)
8a. NAME OF FUNDING/SPONSORING ORGANIZATION: U.S. Army Medical Research & Development Command; 8b. OFFICE SYMBOL (If applicable)	9. PROCUREMENT INSTRUMENT IDENTIFICATION NUMBER: DAMD17-88-C-8133
8c. ADDRESS (City, State, and ZIP Code): Fort Detrick, Frederick, Maryland 21701-5012	10. SOURCE OF FUNDING NUMBERS: PROGRAM ELEMENT NO. 63002A; PROJECT NO. 3M2-63002D807; TASK NO. AH; WORK UNIT ACCESSION NO. 053

11. TITLE (Include Security Classification)
(U) Coxiella burnetii Vaccine Development: Lipopolysaccharide Structural Analysis

12. PERSONAL AUTHOR(S)
V. N. Reinhold

13a. TYPE OF REPORT	13b. TIME COVERED	14. DATE OF REPORT (Year, Month, Day)	15. PAGE COUNT
Midterm	FROM 9/26/88 TO 9/25/89	1989 December 29	47

16. SUPPLEMENTARY NOTATION

17. COSATI CODES		
FIELD	GROUP	SUB-GROUP
07	03	
06	01	

18. SUBJECT TERMS (~~Continue on reverse if necessary and identify by block number~~)
~~RA-14~~ Lipopolysaccharide; Immunogen; Coxiella burnetii. (TES)

19. ABSTRACT (Continue on reverse if necessary and identify by block number)

This Midterm report details new analytical approaches developed for the determination of endotoxin structures at much improved sensitivity and specificity, and an application of those techniques to Coxiella burnetii LPS. Foremost in this methodology is a reducing-end reagent synthesized to provide femtomole (10^{-15}) detection for O-antigen oligosaccharides. A second development focuses on methodology to extract the details of linkage, branching, and sequence, by periodate oxidation, supercritical fluid chromatography, and mass spectrometry. These techniques combine to provide the elements of a global approach to oligosaccharide structure. The utility of supercritical fluid chromatography for a determination of Lipid-A from Salmonella minnesota has been demonstrated. Finally, the structural features of Lipid-A from Coxiella burnetii is described using a combination of these newly developed analytical techniques.

20. DISTRIBUTION/AVAILABILITY OF ABSTRACT	21. ABSTRACT SECURITY CLASSIFICATION
☐ UNCLASSIFIED/UNLIMITED ☒ SAME AS RPT. ☐ DTIC USERS	Unclassified

22a. NAME OF RESPONSIBLE INDIVIDUAL	22b. TELEPHONE (Include Area Code)	22c. OFFICE SYMBOL
Mary Frances Bostian	301-663-7325	SGRD-RMI-S

DD Form 1473, JUN 86 — Previous editions are obsolete. — SECURITY CLASSIFICATION OF THIS PAGE

FOREWORD

Opinions, interpretations, conclusions and recommendations are those of the author and are not necessarily endorsed by the US Army.

✓ Where copyrighted material is quoted, permission has been obtained to use such material.

✓ Where material from documents designated for limited distribution is quoted, permission has been obtained to use the material.

✓ Citations of commercial organizations and trade names in this report do not constitute an official Department of Army endorsement or approval of the products or services of these organizations.

✓ In conducting research using animals, the investigator(s) adhered to the "Guide for the Care and Use of Laboratory Animals," prepared by the Committee on Care and Use of Laboratory Animals of the Institute of Laboratory Resources, National Research Council (NIH Publication No. 86-23, Revised 1985).

✓ For the protection of human subjects, the investigator(s) adhered to policies of applicable Federal Law 45 CFR 46.

✓ In conducting research utilizing recombinant DNA technology, the investigator(s) adhered to current guidelines promulgated by the National Institutes of Health.

Duncan L. Reed 12/29/89
PI - Signature DATE

TABLE OF CONTENTS

I. INTRODUCTION

The complications of vaccine development can be related, in large part, to a lack of understanding LPS structure and its underlying cause, the woeful state of glycolipid and oligosaccharide analytical methodology. As a consequence, an unknown structure brings forth a problem of research focus: (i) to utilize established methodology and grind out results that demand an inordinate amount of material; or (ii) invest in a research approach focused on methods development with the hope of improving methodology in this difficult area.

Throughout this contract we have pursued both activities, introducing new instruments and methodology whenever it seemed to offered some hope of success, and challenging these techniques with two LPS samples, a known structure from Salmonella minnesota, and an unknown LPS from Coxiella burnetii. In this late Midterm Report, (selected aspects detailed in previous reports), we discuss these developments and apply the methodology to these two LPS samples. This report summarizes that effort and introduces a global approach to the sequence determination of carbohydrate materials and defines the major structural elements of Coxiella burnetii Lipid-A.

II. METHODS DEVELOPMENT:

A. O-ANTIGEN DETECTION AT FEMTOMOLE SENSITIVITY

a.) Introduction

The difficulty of detection during chromatographic separation of carbohydrate materials has been frequently addressed by one of two techniques: (i) pre-column reducing-end conjugation with fluorescent or UV-absorbing groups (1-5); and more recently, (ii) post-column amperomeric detection of base ionized samples (6,7). Reducing-end conjugation has involved either reductive amination (2) or direct glycosylation (5). This later technique provides improved column resolution, when compared to reduced samples (5), and, as described below, important advantages for subsequent chemical manipulations. Both conjugated products are well suited for analysis by fast-atom bombardment (FAB) because of terminal charge localization and improved sensitivity (3,4,8). This sensitivity, however, still falls short of that routinely available for other biopolymers. Moreover, the primary sequence derived is wholly inadequate for complete oligosaccharide characterization. For this reason alternative procedures were investigated to improve O-antigen and oligosaccharide detection.

Halogenated materials, or samples prepared as such, have proven most successful in extending detection limits when coupled with negative ion chemical ionization (NCI). A specific example of this approach was demonstrated for derivatized prostaglandin samples, using electron capture detection (9-11) and NCI-MS (12-15). In an effort to bring comparable sensitivity to the structural problems of Coxiella burnetii, we have developed and describe a derivative which imparts improved chromatographic properties, appropriate chemistry for O-antigen and oligosaccharide conjugation, facile negative-ion chemical ionization (NCI) lability for maximum MS sensitivity, and aromatic character for anionic charge stabilization.

b.) Synthesis of Pentafluorobenzylaminobenzoate (PFBAB)

One hundred milligrams of para-amino benzoic acid (PABA)

were dissolved in 2 ml of acetonitrile followed by the addition of 200 µl of pentafluorobenzyl bromide and 500 µl diisopropylethylamine. The mixture was vortexed and allowed to sit 10 minutes at room temperature and the solvents were evaporated under vacuum. The PFBAB product was purified by preparative C-18 HPLC, using isocratic elution with acetonitrile and water (58:42) as the solvent.

These procedures were essentially those first reported by Wickramasinghe, et al., for the derivatization of prostaglandin $F2_{\alpha}$ (11).

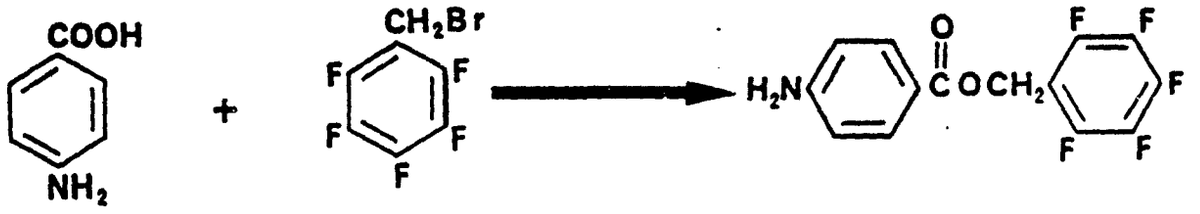

PABA + PFBBr ----------> PFBAB

These workers modified the earlier derivatization procedures for phenols, mercaptans (9) and organic acids (10) by using acetonitrile as the solvent and introduced diisopropylethanolamine as the hindered base. Several recent reports have continued to use the same general derivatization procedures (12-15) using negative-ion chemical ionization mass spectrometry. The conditions described in this report are a simple scale-up of the earlier work (11) without heating and longer reaction times. The product yields were evaluated by both HPLC and GLC. Minor peaks appear in both chromatograms which were analyzed by mass spectrometry. The spectra of these minor fractions could be accounted for as pentafluorobenzylation products of the free amine group on PFBAB and the unreacted free acid, PABA. These extraneous components were in such low concentration, and easily resolved by HPLC, that no attempt was made to diminish their accumulation by modifying the reaction conditions. The HPLC-purified PFBAB product exhibited a UV absorption maxmium, λ_{max}, at 293 nm with a minor red shift following glycosyl conjugation, (Fig. 1a). Using this absorption maximum, the extinction coefficient (ε) of PFBAB was determined to be 2.0×10^4 M^{-1} cm^{-1} and 1.9×10^4 M^{-1} cm^{-1} for the fucose glycosylated derivative. The concentration of the latter derivative was determined by GLC. The UV detection limits were determined to be 1.6 µMolar, ($\varepsilon/n = 10$). Using a similar approach, the pyridinylamine (PA) derivative of fucose was determined to have an $\varepsilon = 0.8 \times 10^4$ M^{-1} cm^{-1}, indicating less sensitive detection limits. The PA-fucose derivative was measured at its absorption maximum of 232 nm.

The PFBAB reagent was also found to be fluorescent. The fucose derivative provided a $\lambda_{max} = 350$ nM upon excitation, ($\lambda_{ex} = 296$ nM), (Fig. 1b). Based on fluorescent scans of equal molar solutions, the PFBAB-fucose was a better fluorophor than PA-fucose by roughly two orders of magnitude. As expected, fluorescence monitoring extended the detection limits of PFBAB-fucose, in this case from 1.6 µM for UV

Figure 1

1a

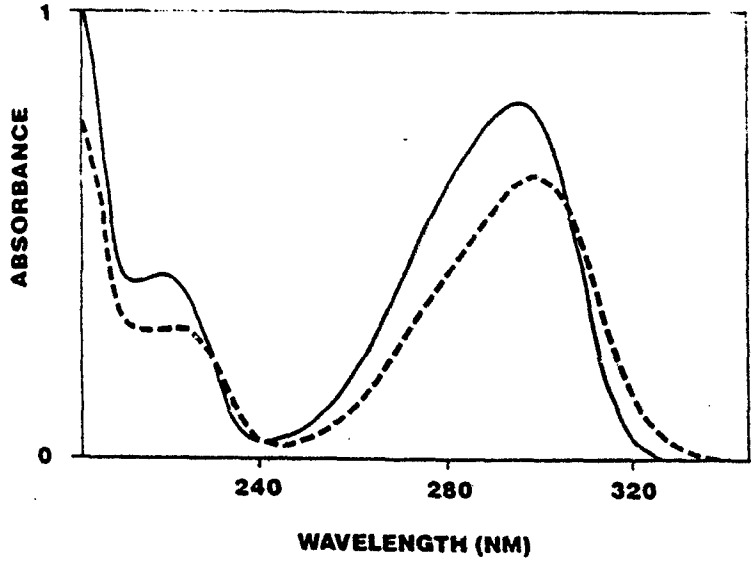

1b

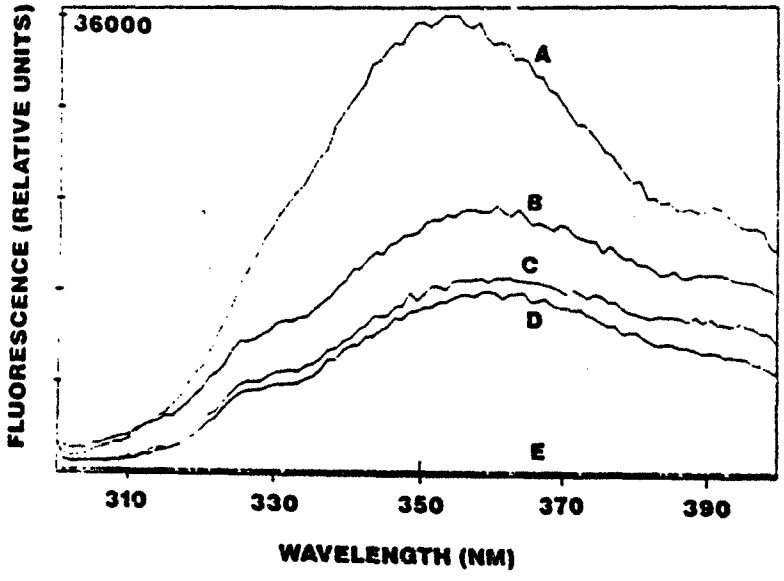

monitoring, to 24 nM for fluorescence monitoring; an approximate 60 fold increase in detectability. Both detection limits were taken from fluorescence scans with signal to noise ratio of about 10/1. By HPLC the UV detection limits of the injected PFBAB-fucose was found to approximate 8 ng, (17 pmoles. The quantum yield (Q) of PFBAB was determined to be 0.04 using L-tryptophan as a reference standard, (Q = 0.13).

c.) Oligosaccharide Glycosylation With PFBAB

One hundred micrograms of a reducing (free reducing-end) oligosaccharide was solubilized in a reaction vial with 50 μl of a 1:1 mixture of methanol and acetic acid. To this clear solution was added a 10 molar excess of the PFBAB reagent in 25 μl of the same solvent. The 75 μl volume was sealed (Teflon-lined screw tops) and heated for 20 min at 65 ^{o}C. The reaction vessel was brought to room temperature and dried by vacuum centrifugation. For sample storage, and to remove all traces of acetic acid, the tubes were twice dissolved in methanol and dried. The reaction was followed and yields determined by SFC following peracetylation. Supercritical fluid chromatography, and peak area integration, provides a measure of yield as determined by reactant/product ratios, which under these conditions were always greater than 90%.

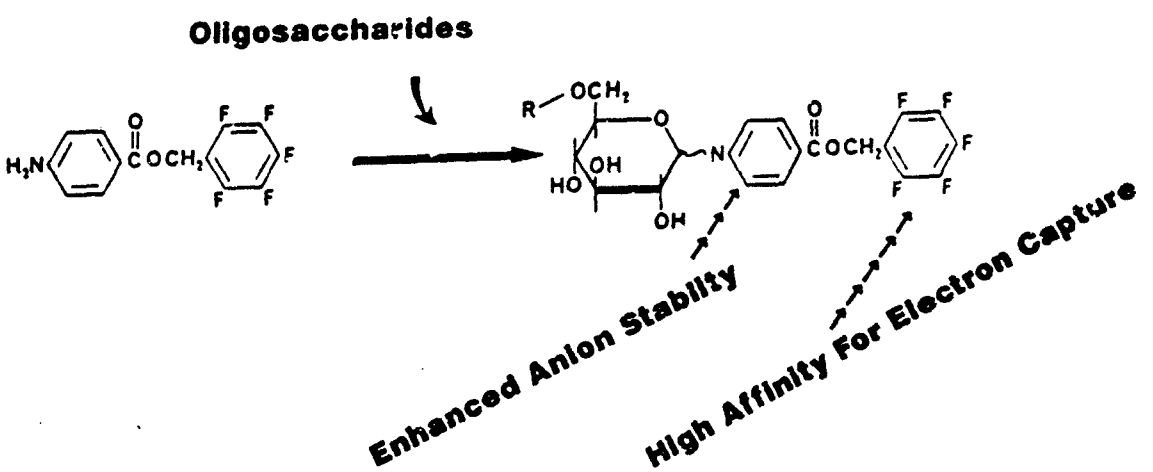

Preliminary conditions for PFBAB glycosylation were initiated using established procedures (5) and fucose as a model compound. The low molecular weight product could be acetylated for easy analysis by GLC. Extension of these conditions to oligosaccharides was facilitated by SFC which allowed both reactant and product evaluation via flame ionization detection. Increased product yields were a combination of achieving reactant solubility while avoiding product degradation. Although aqueous acidic solvents were most effective for solubilizing larger glycans, they were more prone to degradation with reaction time. Non-aqueous conditions with acetic acid-methanol solvents proved most successful. The solvent polarity was adequate for bringing glycans into solution and, under the reaction conditions established, degradation was undetected. To

evaluate this latter point, the loss of a labile group, (neuraminic acid), from glycans was evaluated. It was noted that this acid (both 3- and 6-linked) was not lost from the trisaccharide, neuraminyllactose, nor from α_1-acid glycoprotein under the PFBAB derivatization conditions. The kinetics of PFBAB conjugation can be followed by SFC which allows a determination of products and reactants in each analysis using FID detection. For small saccharides (dp = 2 - 7) derivatization is quantitative, but with larger oligomers, 20 minutes was insufficient (Fig. 2). When PFBAB glycosylation was applied to a mixture of N-linked high-mannose glycans obtained from a plant glycoprotein, the product yields decreased, but approached quantitation with longer reaction times and/or higher temperatures. Different classes of oligosaccharides will undoubtedly have to be evaluated separately to maximize yields. From these limited studies, however, it does appear that the chemistry of PFBAB glycosylation with hexoses and amino sugars proceeds satisfactorily, and under conditions that insure product stability. Although somewhat less than quantitative, the striking increase in sensitivity achieved by PFBAB glycosylation and NCI-MS (see below) greatly offsets these small losses in derivatization.

d.) Negative Ion Chemical Ionization MS Sensitivity

Min, et al., (12) using the PFB derivative and single-ion monitoring, [$(M - C_7H_2F_5)^-$, NCI-MS] had indicated sensitivities for prostaglandin $F2_\alpha$ approximating 1 pg (injected). This value was reported to be five times better than electron capture detection (EC-GLC) and twenty-five times better then a completely silylated derivative, $(M - TMSOH)^-$. Similar comparisons between NCI and positive EI have been reported and the striking stability of the carboxylate anion noted (15). In a preliminary effort, to access the limits of detectability, the PFBAB-fucose derivative was analyzed by SFC-NCI-MS using full mass spectral scans (100 - 1000 Da) (16). Using a series of dilutions, injection of 55 femtomoles provided an abundant signal for the $(M - C_7H_2F_5)^-$ fragment. No total ion current was detected at this level, however, an ion plot [$(m/z\ 408, M - C_7H_2F_5)^-$] provided one major peak with a s/n = 10, Fig. 3. Sensitivity studies at higher mass has provided comparable data. Presented in Figure 4 is the total ion plot of a complex mixture of glycans isolated from a plant, labeled with PFBAB and analyzed by SFC-NCI-MS. Recessed to the right in this figure are a series of ion plots representative of each component comprising the mixture separated by these mass chromatograms.

The extraordinary sensitivity developed with these techniques can be attributed to several factors. Most important, and as observed by others (12-15), is the unique character of the PFB moiety to serve as an efficient electron trap. The high electronegativity of F leads to a lowering of the lowest unoccupied molecular orbital energy and thus an increase of electron affinity. The resident negatively charged PFBAB residue is than stabilized by ester bond rupture to leave, in high abundance, the carboxylate anion. Secondly, is the level and distribution of fragmentation energy which is adequate for ester rupture only and not dispersed into alternative fragmentation pathways. Thirdly, is the unique stability of the carboxylate anion. These factors combine to provide excellent detecting sensitivity.

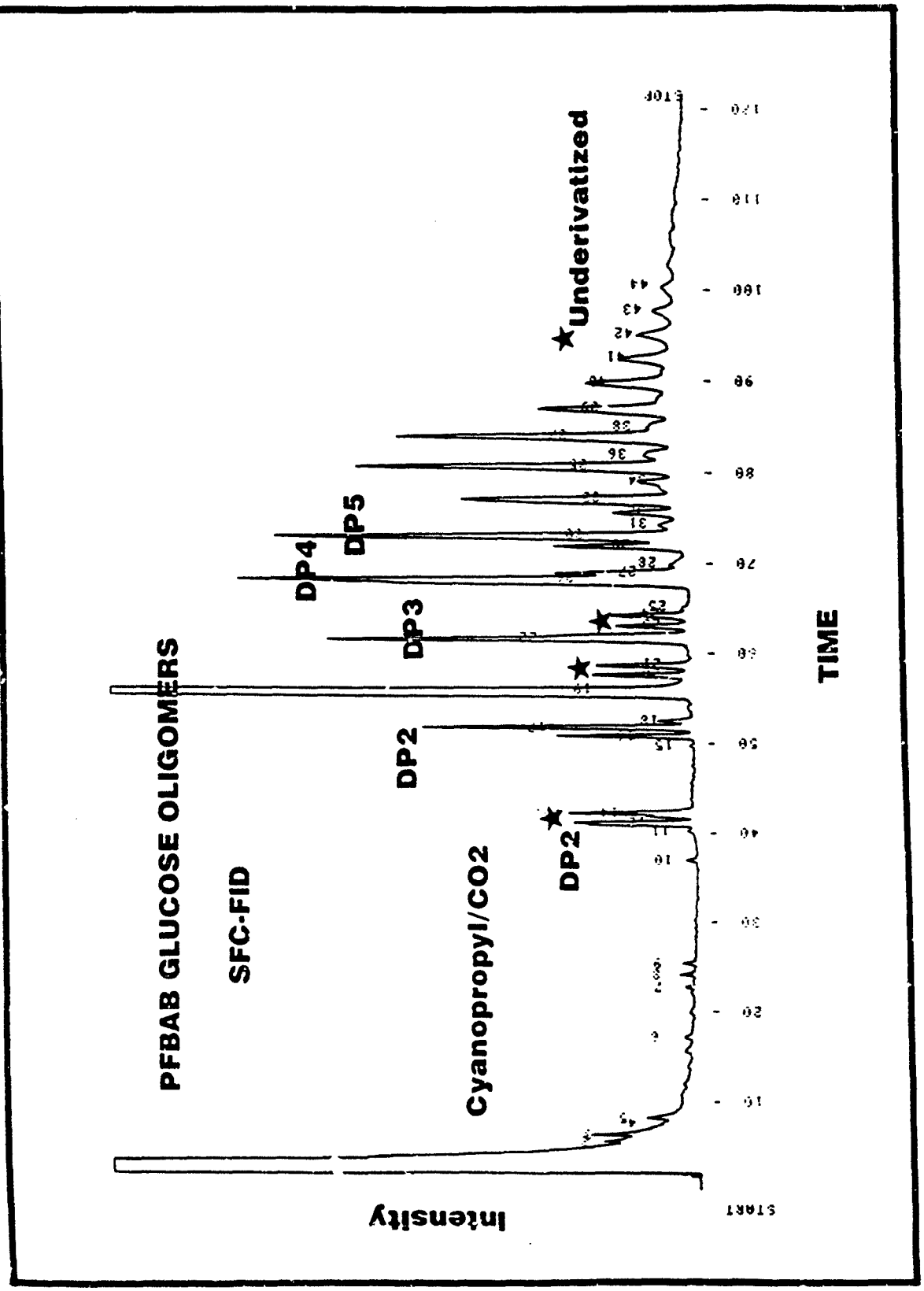
PFBAB GLUCOSE OLIGOMERS
SFC-FID
Cyanopropyl/CO2
Intensity
TIME
START
DP2
DP2
DP3
DP4
DP5
Underivatized

Figure 2

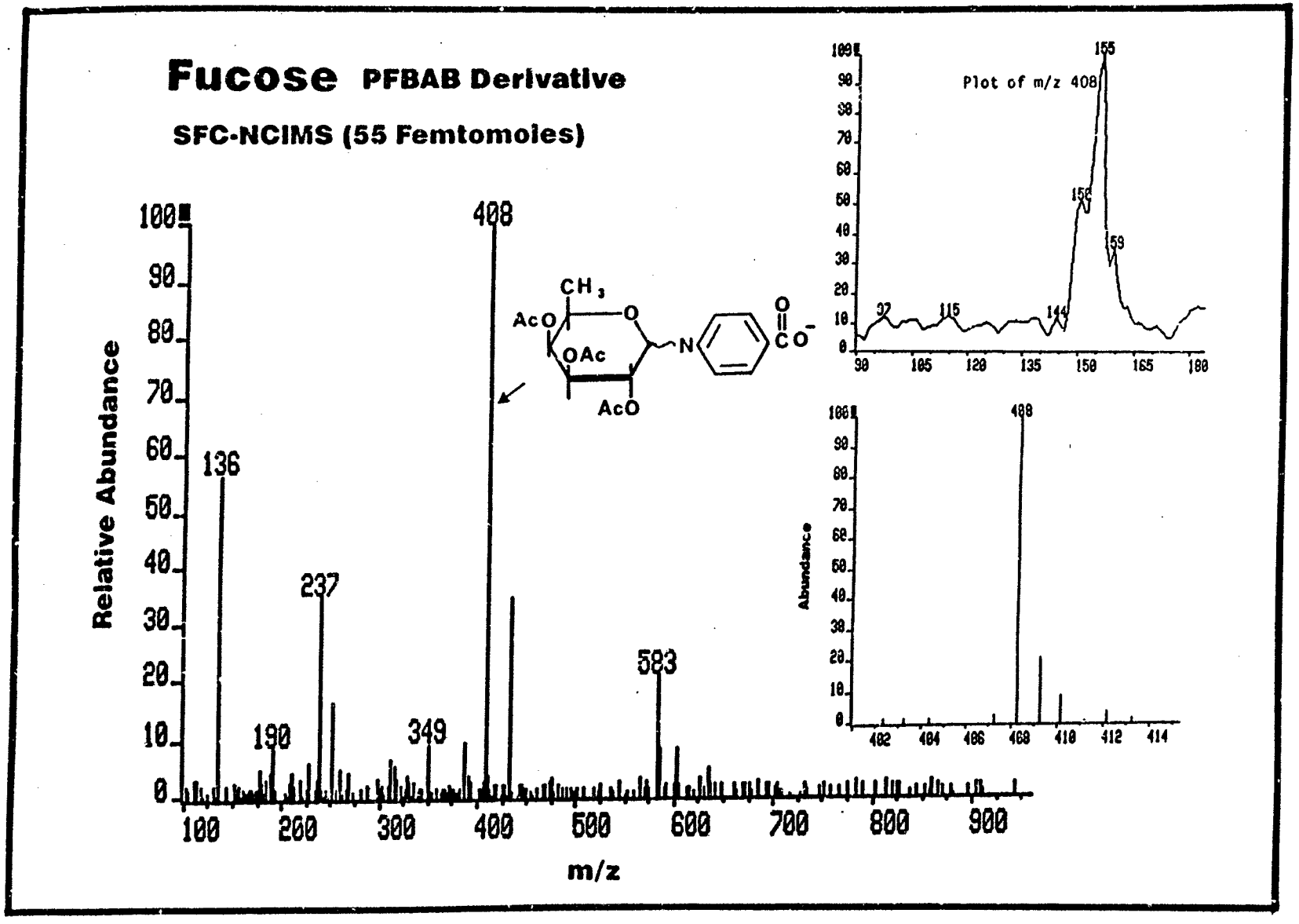
Fucose PFBAB Derivative
SFC-NCIMS (55 Femtomoles)
Relative Abundance
m/z
136
190
237
349
408
583
Plot of m/z 408
155
156
159
97
115
144
Abundance
408
CH3
AcO
OAc
AcO
O
N
O
CO-

Figure 3

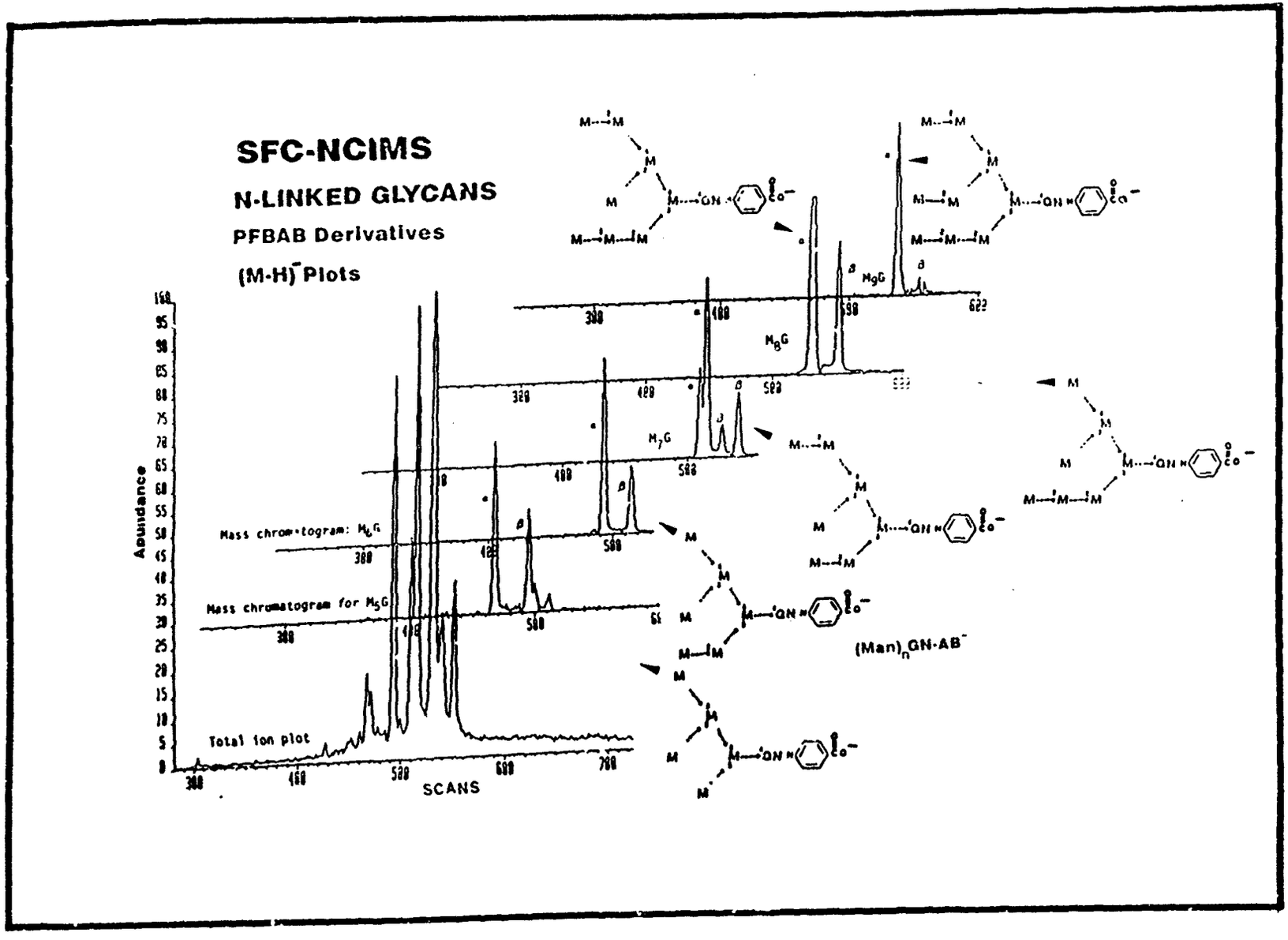
SFC-NCIMS
N-LINKED GLYCANS
PFBAB Derivatives
(M-H)⁻ Plots
Abundance
Mass chromatogram: M6G
Mass chromatogram for M5G
Total ion plot
SCANS
M8G
M7G
M6G
(Man)nGN-AB⁻

Figure 4

B. LINKAGE, SEQUENCE & BRANCHING

The procedures described above, (which were developed to maximize sensitivity), provide a molecular weight analysis with little structural detail. In fact, the soft ionization of SFC-NCI is a major factor that contributes to this excellent sensitivity. Sequence, linkage and branching detail, however, can not be obtained from this analysis. Classically, this problem is approached by sample permethylation, hydrolysis and acetylation with the products analyzed by gas chromatography and mass spectrometry, (e.g., alditol acetate procedure). Unfortunately, this approach provides only a composition of linkage type, not linkage data in a sequential array.

a.) Periodate Oxidation

To approach the problem of determining monomer linkage, we have introduced a series of chemical steps to impart greater molecular specificity.

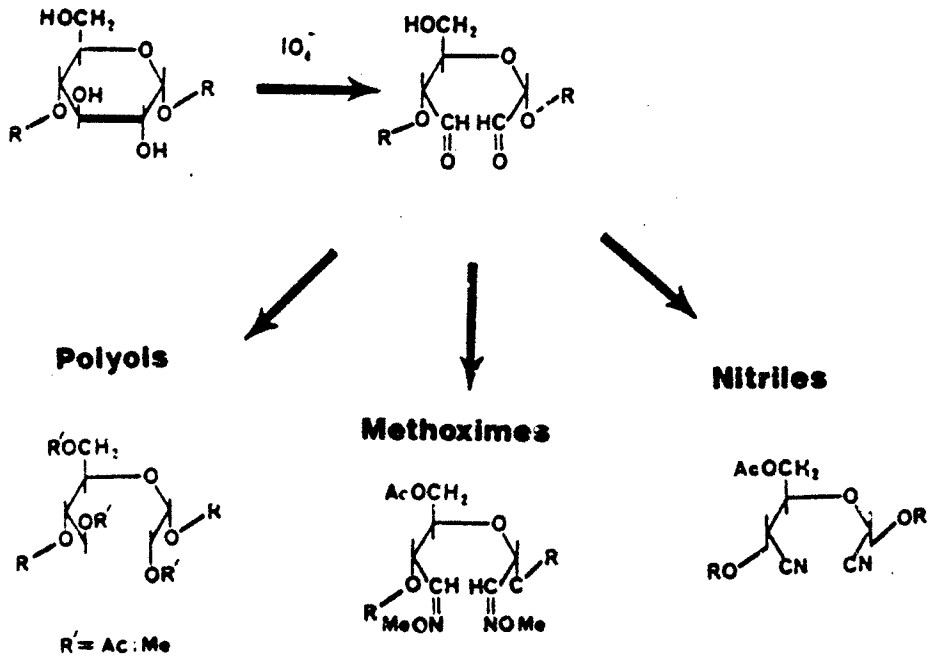

From these structural modifications intervening moiety linkage can be determined. The reasons for this can be explained by considering the change in the residue molecular weight upon oxidation and aldehyde derivatization, Scheme 1. Inter-residue linkages that leave adjacent hydroxyl groups are subject to oxidation, thus, periodate oxidation of 2-, 4-, and 6-O-linked moieties, (3-O-linked unaffected) result in different structural products which contribute variations in structure and changes in glycan molecular weight. Periodate oxidation, reduction and permethylation has been utilized by Nilsson, et al., (17) for samples studied by FAB-MS. For the aldehyde derivatization step, we have investigated several derivatives to

Interval Residue Molecular Weights

Methoximes

1---6

Residue MW

188 pyran
260 furan

1---4

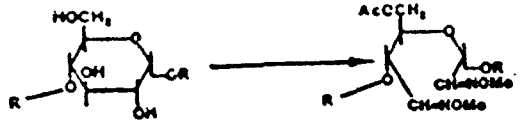

260 pyran

1---3

288 pyran
201 furan

1---2

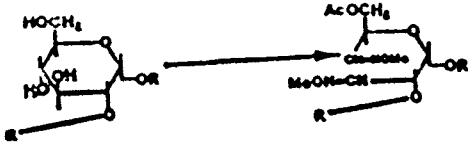

260 pyran
201 furan

POLYNITRILE GLYCOSIDES

1--6

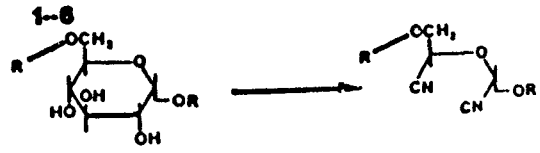

Residue MW

124 pyran
196 furan

1--4

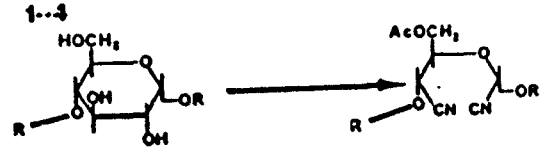

196 pyran

1--3

288 pyran
169 furan

1--2

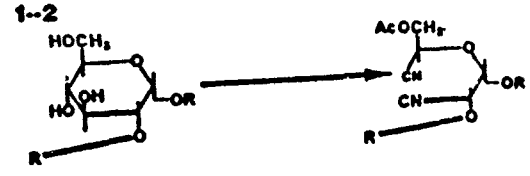

196 pyran
169 furan

Scheme 1

capture the products of periodate oxidation. At present, the chemistry appears to be more quantitative and the fragmentation following CID, (see below), more structurally informative when using the O-methyl oxime derivative. In addition to providing greater insight on linkage, there is information on furan/pyran structure. From the summation of residue molecular weight changes, a linkage composition analysis can be ascribed. The experimental conditions of oxidation and aldehyde derivatization has been established with di- and trisaccharides of different linkage type and more recently with highly branched N-linked glycans and oligosaccharides.

Fast atom bombardment mass spectrometry has been utilized to follow the chemistry. Presented in Figure 5 is the FABMS of a highly branched oligosaccharide periodate oxidized and conjugated with methoxamine. The spectral and molecular weight information provided by this analysis indicates the chemistry to be correct and quantitative. We have investigated other complex PFBAB-labeled oligosaccharides by SFC-NCI-MS with comparable results, Fig. 6. The application of this methodology to the O-antigen obtained from Coxiella burnetii hydrolysates is under investigation.

b.) Collision Induced Dissociation

An important follow-up of this chemical strategy would be to capture the inner-residue molecular weight changes in addition to the total molecular weights obtained by FAB. This can be done by collision induced dissociation (CID). We have previously reported on the structural determination of the O-antigen from Coxiella burnetii using CID. This technique allows the selection of parent ions and focuses these molecular weight-related materials into a collision cell that induces fragmentation at glycosidic linkages yielding oligomer sequence and branching. Combining CID with the periodate chemistry described above would provide for the first time an inner residue linkage assessment for oligosaccharides. As a summation of the chemical and instrumental techniques introduced in this Midterm Report, we would wish to indicate their potential significance when applied to a problem; the structural characterization of two highly branched oligosaccharide isomers, Man_7GN-PFBAB, Fig. 7. Although we have already resolved these structures by conventional methods, (using large amounts of material), and several weeks; it may now be possible to arrive at the same structural result with picogram amounts of sample and a few hours. The Figure illustrates the expected MS-CID spectra, that could be expected from each isomer following PFBAB-derivatization, periodate oxidation, aldehyde trapping and acetylation, (in this example we considered the sample to be prepared as the nitrile instead of the O-methyloxime....this would change the masses, but the relative shifts would be unchanged). The fragments speculated are limited to only those of labile glycosidic cleavages, and although it is easy to see spectral differences there is a wealth of information in each of the fragments indicating linkage, furan-pyran relationships and branching. Thus, these techniques introduce the possibility of glycan sequencing at enhanced sensitivity using periodate oxidization, reagent-labeling, and instrumental analysis by SFC-NCI and MS-CID.

C. ENDOTOXIN CHARACTERIZATION BY SFC

The characterization of Lipid-A materials from Gram negative

Figure 5

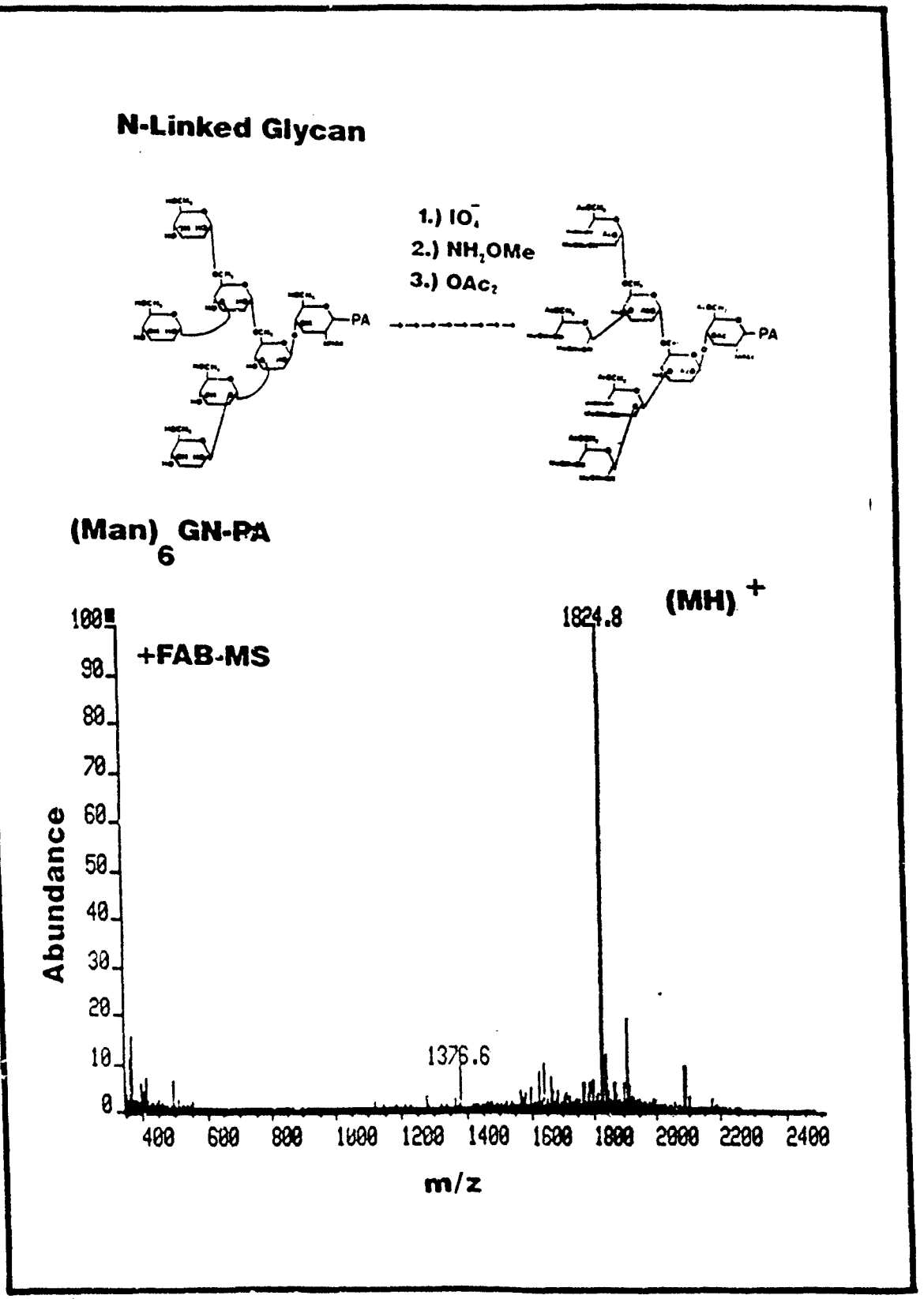
N-Linked Glycan
1.) IO_4^-
2.) NH_2OMe
3.) OAc_2
PA
PA
(Man)$_6$ GN-PA
(MH)$^+$
1824.8
+FAB-MS
Abundance
100
90
80
70
60
50
40
30
20
10
0
1376.6
400
600
800
1000
1200
1400
1600
1800
2000
2200
2400
m/z

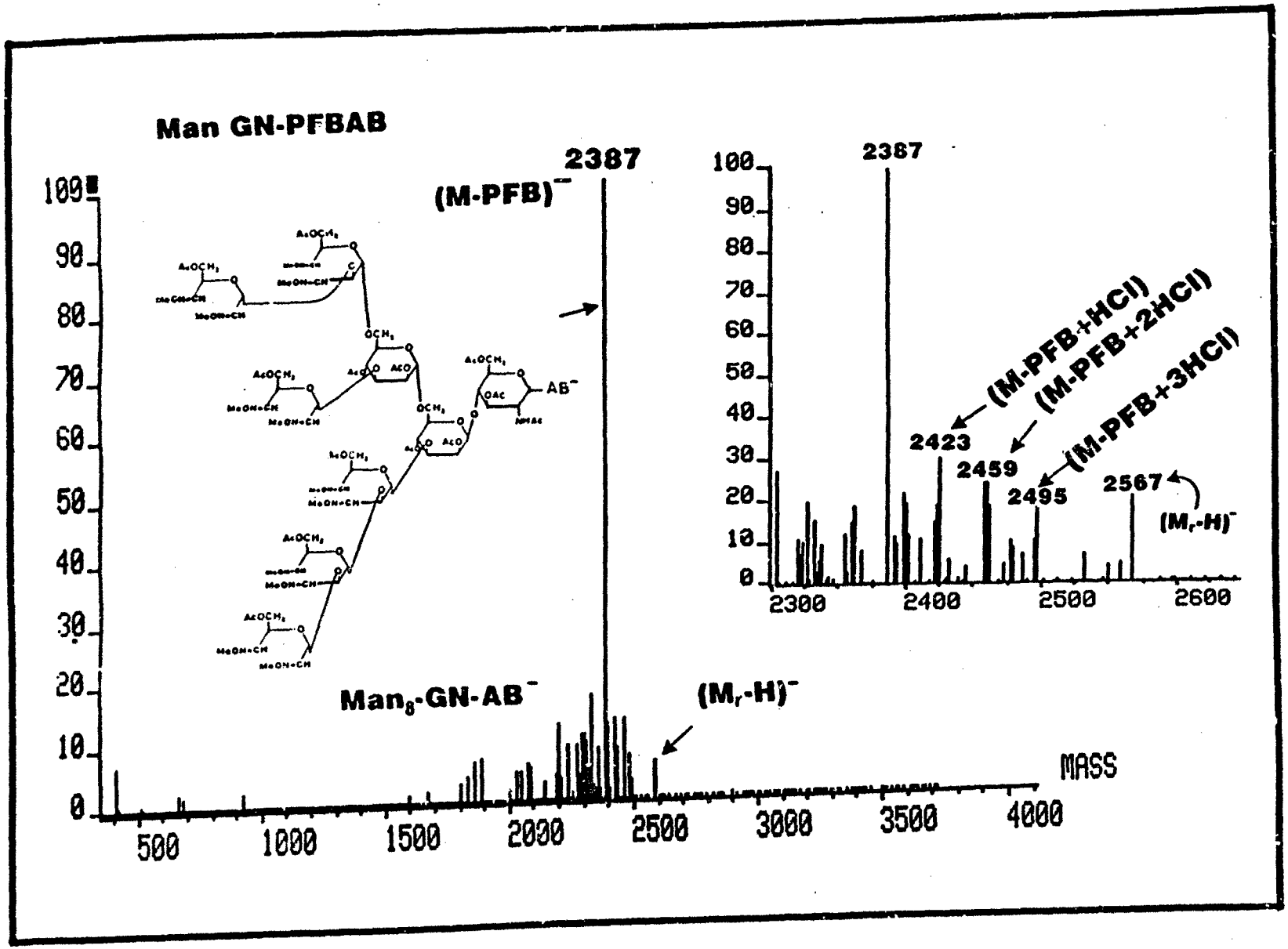
Man GN-PFBAB
2387
(M-PFB)⁻
AB⁻
Man8-GN-AB⁻
(Mr-H)⁻
MASS
100
90
80
70
60
50
40
30
20
10
0
500
1000
1500
2000
2500
3000
3500
4000
2387
(M-PFB+HCl)
(M-PFB+2HCl)
(M-PFB+3HCl)
2423
2459
2495
2567
(Mr-H)⁻
2300
2400
2500
2600

Figure 6

POLYNITRILE GLYCOSIDES MS-CID-MS

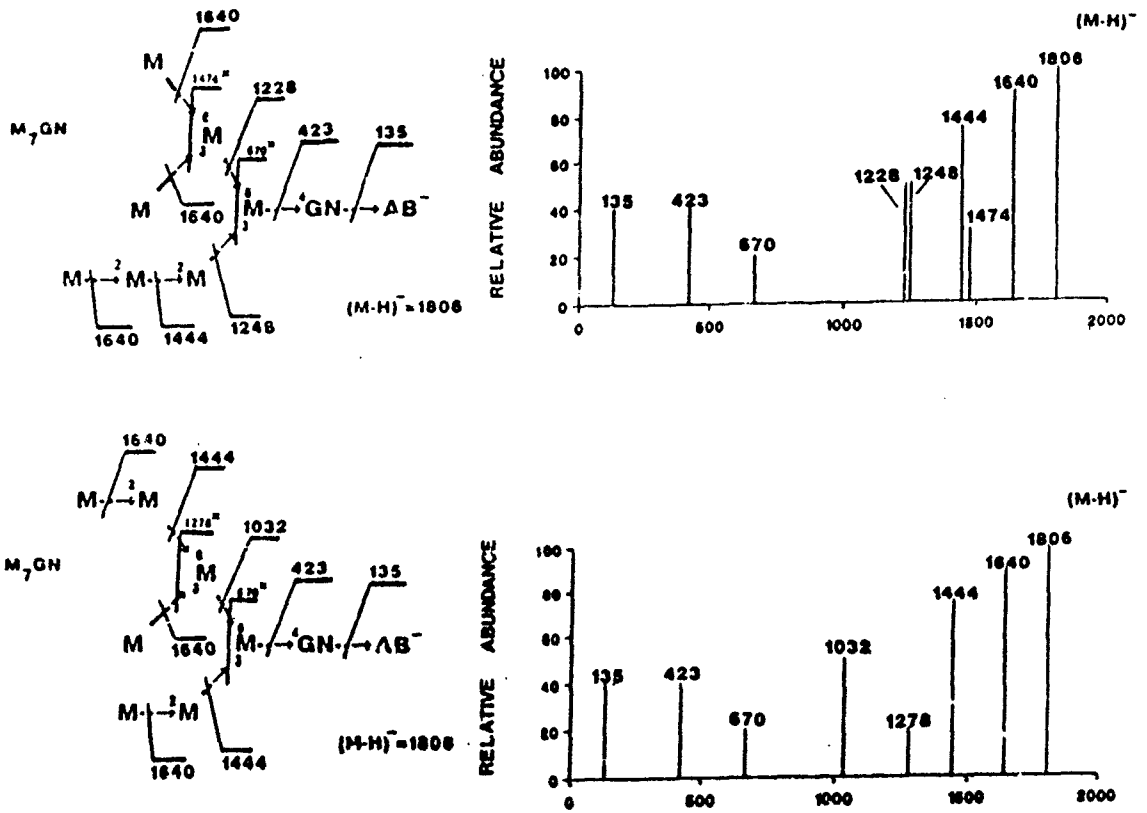

Figure 7

bacteria has, over the years, been a most demanding and challenging analytical problem. We introduced SFC to assist in the study of Coxiella burnetii LPS fractions, and with known glycolipid and oligosaccharide samples, developed separation parameters and a mass spectrometer interface for product characterization. The direct application of this instrumentation to Coxiella burnetii LPS has been thwarted by the earlier difficulties of partial degradation to release sufficient amounts of material for study. The value and power of this analytical approach is directly demonstrated in this section with the multi-component mixture obtained from Salmonella minnesota LPS. We have separated by TLC, extracted, and studied by FAB-MS all the entities comprising this Lipid-A sample (18). This preliminary effort has aided in the development of chromatographic parameters to separate this complex mixture by SFC. Presented in Figure 8 is an SFC chromatogram of the Lipid-A components detected in the partial hydrolysate of LPS obtained from Salmonella minnesota R595. The identification of these SFC peaks relates to our earlier study by TLC and FAB-MS. We are currently completing these studies by direct SFC-MS and SFC-MS-CID-MS.

III. COXIELLA BURNETII LPS CHARACTERIZATION:

A. EXPERIMENTAL

a.) Mass Spectrometry

Fast atom bombardment mass spectrometry (FABMS) was performed on a VG ZAB-SE instrument (VG Analytical, Manchester, UK) operated at 8 and 10 kV in the negative and positive modes, respectively. The Ion Tech gun was operated at 8 kV with 1 mA of current at the cathode; xenon was used as the FAB gas. Current controlled scans were acquired at a rate of 30 sec/decade, and 3-5 scans were summed as continuous data before converting to bar plots using the VG 11-250 data system. The resolution was typically 1:2000; CsI clusters were used for calibration. For positive FABMS, the matrix was a mixture of 1:1 meta-nitrobenzyl alcohol (MNBA) and thioglycerol, and for negative FABMS, 1:1 MNBA and triethanolamine was used. Direct chemical ionization mass spectrometry (DCIMS) was performed by depositing sample on a platinum wire, and heated at a rate of 16 mA/sec in an ammonia plasma with a source housing pressure of 1 x 10^{-4} mbar. Mass analyzed ion kinetic energy spectra (MIKES) were acquired by focusing the beam of FAB-generated ions into the collision cell in the second field-free region, and scanning the electric sector at a rate of 30 sec/scan. Helium was admitted into the collision cell at a pressure sufficient to attenuate the precursor beam to 30-50%.

b.) Hydrolysis and Methanolysis of Lipopolysaccharides

Hydrolyses of the lipopolysaccharides (LPS) were carried out in 1:1 water:methanol (1-2 mg/ml) at HCl concentrations varying from 0.01 to 0.65 N HCl or 1% acetic acid (vol/vol) at 100 ^{o}C for two hours. A time study was also carried out using 0.04 N HCl in 1:1 water:methanol at 100 ^{o}C for 0.5, 2, and 6 hours. The same HCl acid concentration and time studies were also performed in anhydrous methanol. Methanolysis or methanolic hydrolysis products were extracted in 1:2:4 water (or 0.1 N HCl):methanol:chloroform. There usually were insoluble particulates at the organic-aqueous interface following centrifugation. This was somewhat greater in the methanolic

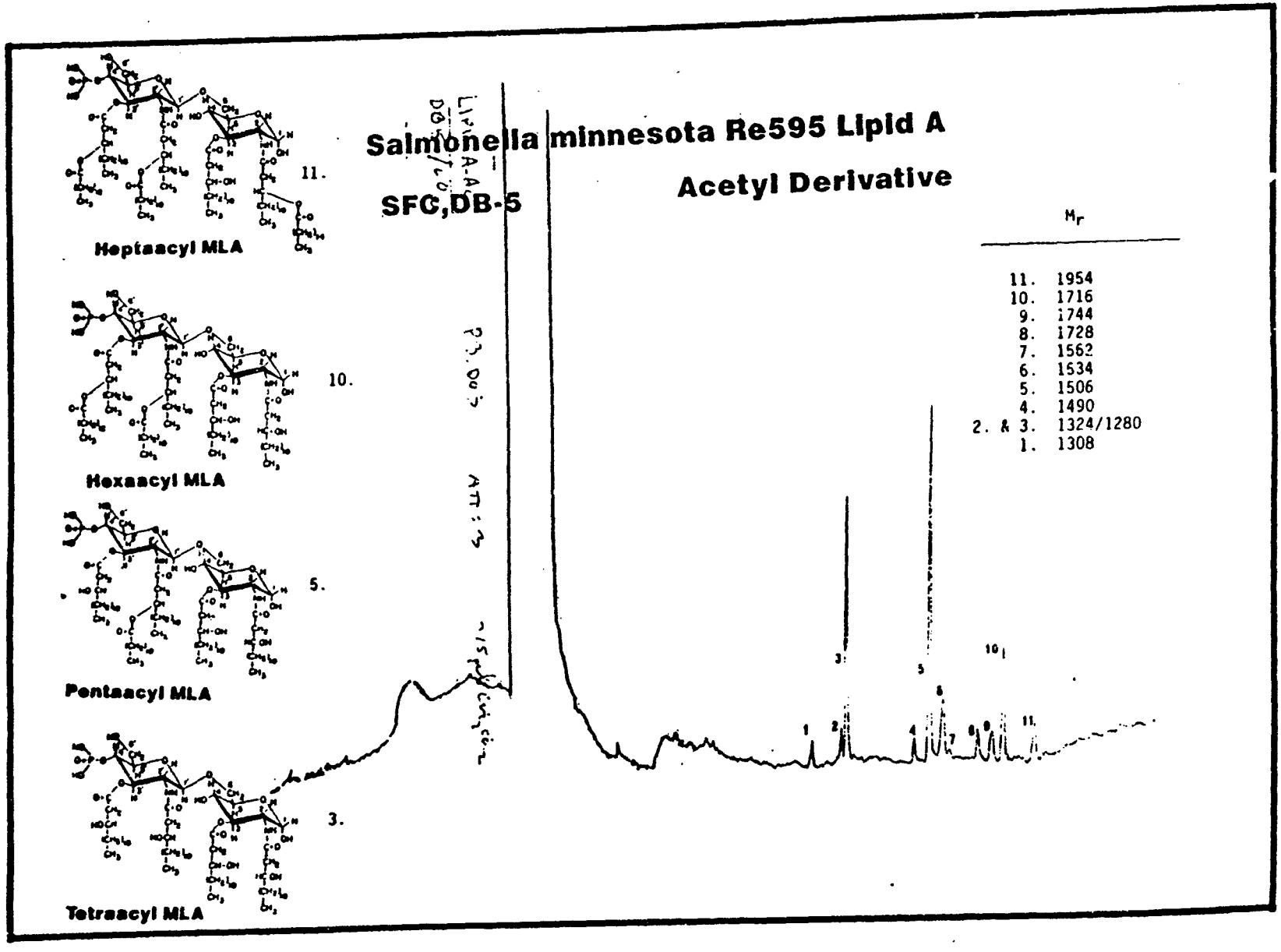
Salmonella minnesota Re595 Lipid A
Acetyl Derivative
SFC,DB-5
Mr
11. 1954
10. 1716
9. 1744
8. 1728
7. 1562
6. 1534
5. 1506
4. 1490
2. & 3. 1324/1280
1. 1308
11.
Heptaacyl MLA
10.
Hexaacyl MLA
5.
Pentaacyl MLA
3.
Tetraacyl MLA

Figure 8

hydrolysis, but was decreased by slight warming of the tubes and extracting with 0.1 N HCl rather than water.

c.) Gas Phase Reduction

A thin coating of the sample was dried onto the bottom centimeter of a capillary melting-point tube, and placed in a gas phase reaction vessel (19). A series of three gas phase reactions were carried out: (i) 0.25 N BH_3 (or BD_3) in THF for 1 hr at 45 °C; (ii) 0.5 N HCl in methanol for 3 hrs at 45 °C; and (iii) 1:1 30% H_2O_2/3 N NH_4OH for 1 hr at 45 °C. The first reaction reduces amides to amines the second step solvates any boronic esters, and the last step oxidizes any carbon-boron bonds that form if any carbon-carbon double bonds are present (20).

d.) Composition Analysis

To characterize the lipophilic anchor and sugar backbone of this lipopolysaccharide, 5 mg of strain 9MIC7 LPS from C. burnetii was subjected to a 0.65 N HCl anhydrous methanolysis (1.25 mg LPS/ml) for 2 hours at 100 °C. The product was dried and extracted four times using 0.1 N HCl:methanol:chloroform 1:2:4, (discarding the top, aqueous layer each time), to insure no contamination from the core or O-antigen regions. To hydrolyze all of the amide bonds, this organic phase was dried and dissolved in 2 µl of THF, suspended in 2 ml of 6 N HCl and heated for 18 hrs at 100 °C. The hydrolysis products were dried, extracted two times with chloroform:0.1 N HCl, 1:1, and the aqueous fraction back extracted twice to remove trace residues of fatty acids. The components in the aqueous fraction were characterized using GLC as the N-acetyl, O-silyl derivative. These derivatives were prepared by dissolving the dried residue, obtained from acid hydrolysis, in 100 µl methanol, 50 µl pyridine, and 50 µl acetic anhydride and holding for 30 min at room temperature. The dried N-acetylated material was silylated in 2:1 pyridine:99% BSTFA + 1% TMCS at room temperature for 45 min. The products were separated on a SE-54 column (Alltech Econocap) using a HP 5890A gas chromatograph. The chromatogram showed three peaks that eluted between 265-275 °C, which were shown to be due to 2,3-diamino-2,3-dideoxy glucose by coinjection with a synthetic standard, (United States Biochemical Corp., Cleveland, OH).

Composition analysis was performed on the intact phase II LPS before and after dephosphorylation with HF (21). Methanolysis (0.65 N HCl) was carried out at 60 °C for 2 hrs, which is optimal for KDO analysis (22); samples were N-acetylated and silylated as described earlier.

e.) Acetylation and De-O-Acylation

Methanolic and methanolic hydrolysis products were peracetylated using 1:1 pyridine:acetic anhydride for 16 hrs at room temperature. Two methods of de-O-acylation were used - triethylamine (10 µl) in water (300 µl) at 100 °C for 15 min, or a saturated ammonia/anhydrous methanol solution at 65 °C for 16 hrs.

f.) Methylation, Diazomethylation, Deuteromethylation

Permethylation was carried out using the NaOH/DMSO method (23). Methylation with diazomethane and deuterodiazomethane was performed by first dissolving the sample in 100 µl of THF and then

adding an ether solution of the reagent until the yellow color appeared indicating completion of the reaction. Deutermethylation was carried out using a deuterodiazomethane generating kit (Diazald, Aldrich Chem. Co., Milwaukee, WI).

B. Results

Isolated Coxiella burnetii LPS samples, hydrolyzed in 1-2% acetic acid or 0.1 N HCl to free Lipid-A moieties, always resulted in large insoluble residues which appeared as a flocculate at aqueous-organic interfaces. Organic phase extracts of these hydrolysates, and mass spectrometrometric analysis using fast atom bombardment ionization, gave no useful fragments for structural characterization. However, when these fractions were highly concentrated and ionized by positive ion direct chemical ionization (DCI, methane as the reagent gas), major ions and fragments were detected at 14 mass unit intervals, which suggested the first clues to a Lipid-A moiety, m/z 640, 658, and 672. No higher mass ions were detected, even at shorter hydrolysis time. This difference in ionization is significant in that the DCI approach is initiated by probe heating, suggesting that the major ions could be products of pyrolysis rather than a consequence of sample hydrolysis. The 14 mass unit interval was also troublesome because such alkane heterogeneity is not observed with Lipid-A from other species. Within a single bacterial species, there are, however, different molecular entities that seem to serve equally as an LPS anchor, and this heterogeneity can usually be attributed to the presence or absence of specific acyl groups (24-27). Most important however is the observation that fatty acids methyl esters derived from Coxiella burnetii Lipid-A fractions yield a distribution of C_{14}, C_{15}, C_{16}, & C_{17} branched hydroxy fatty acids (33) and this ion distribution is comparable with these higher molecular weight samples.

The poor yields of this suspected Lipid-A material focused our attention to alternative acidities and solvents for LPS degradation. The aqueous conditions currently used suggested that the classical conditions are inappropriate for Coxiella burnetii. It was soon observed that more lipophilic solvents greatly increased the abundance of the 658 ion. When these conditions are applied to the LPS obtained from Coxiella burnetii, ions at higher mass were obtained for the first time, m/z 766, 1405 and 2079 (Fig. 9a). At higher acid concentrations (1.5 N HCl), the ion at m/z 751 is predominant while lower concentrations favors the m/z 1405 ion, (Fig. 9b & 9c). Consistent with these differences, it has been reported that higher acylated homologs of Lipid-A were detected from the LPS of Salmonella typhimurium when hydrolysis was carried out in aqueous methanol rather than 100% water (25).

Assuming these ions to be deprotonated molecules, $(M-H)^-$, a relationship between them can be deduced where two molecules of M_r = 752, minus water and a phosphate group equals the molecular weight 1406. The use of a milder acid during hydrolysis, (1% acetic acid rather HCL), resulted in an ion cluster 80 amu higher than the cluster at m/z 1405, [(752 x 2) - (18) = 1486], m/z 1485, (Fig. 10). Thus, from these data, an organic phase component appears to be a dimer associated with two phosphate groups, one somewhat more labile than the other. A decrease in the solvent polarity during hydrolysis followed by lipophilic extraction and FABMS, provided similar ion clusters extended to a tetramer region (Fig. 9a). Other than the

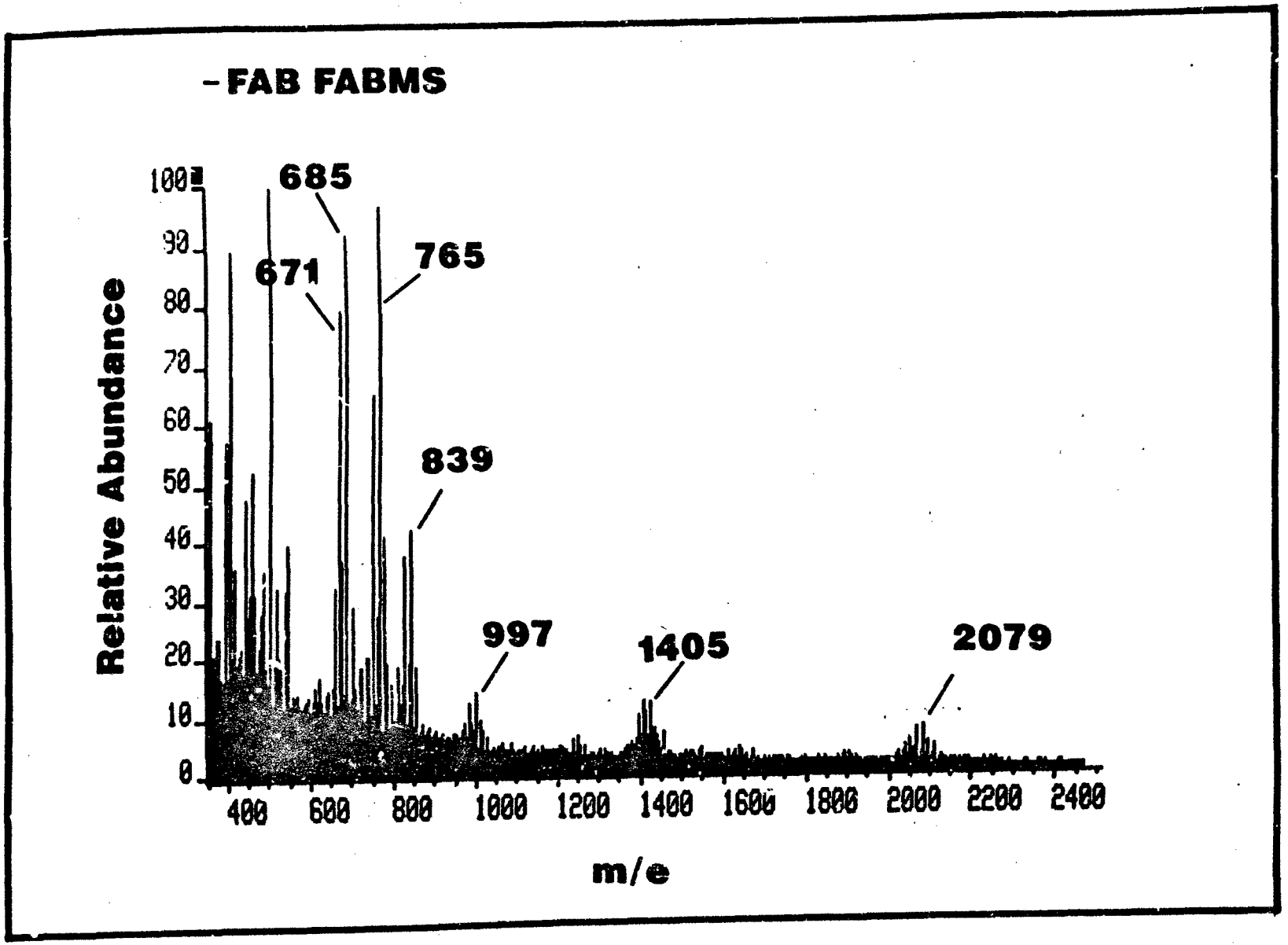
-FAB FABMS
Relative Abundance
100
90
80
70
60
50
40
30
20
10
0
685
671
765
839
997
1405
2079
400
600
800
1000
1200
1400
1600
1800
2000
2200
2400
m/e

Figure 9a

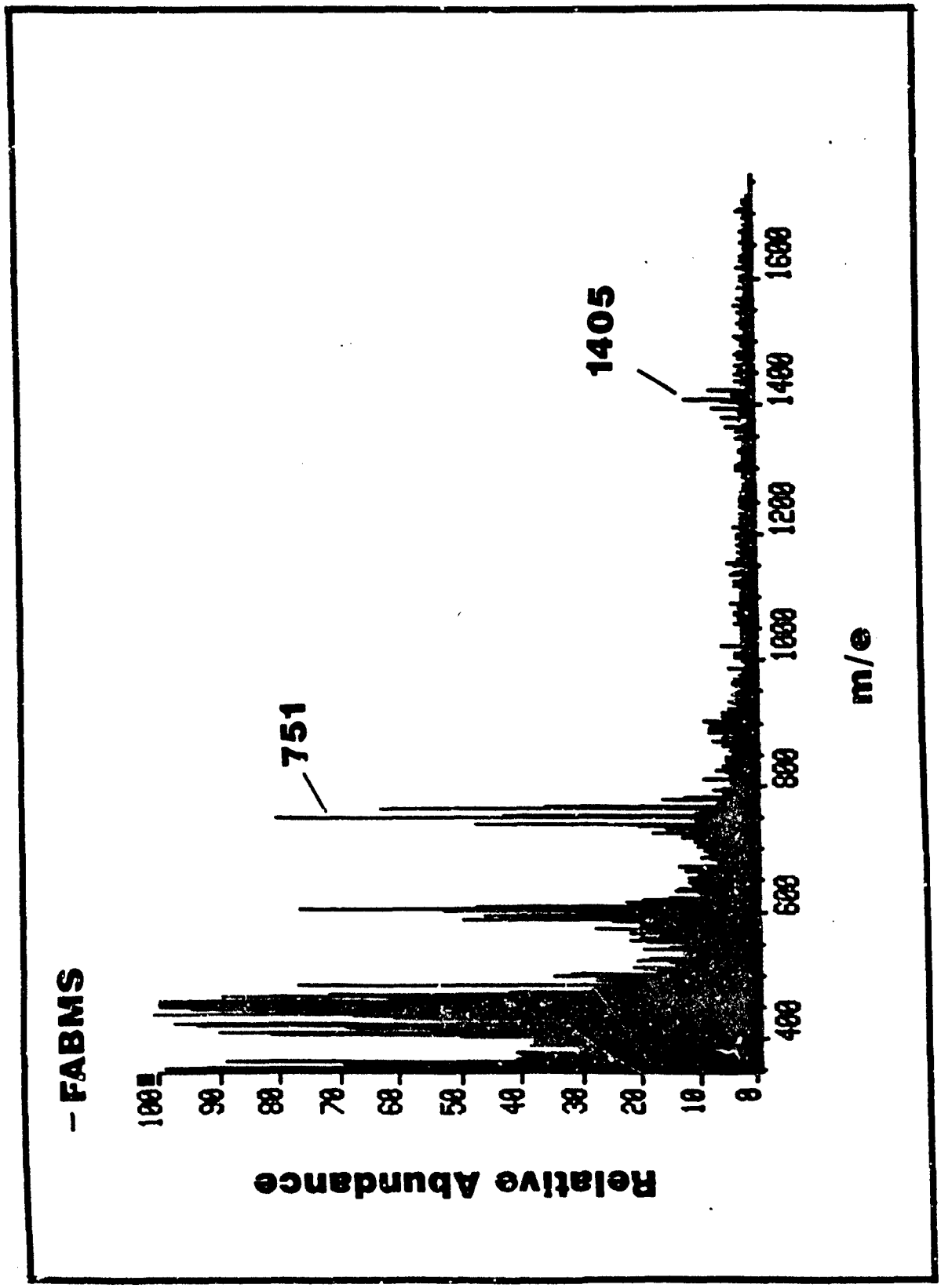
– FABMS
Relative Abundance
100
90
80
70
60
50
40
30
20
10
0
400
600
800
1000
1200
1400
1600
m/e
751
1405

Figure 9b

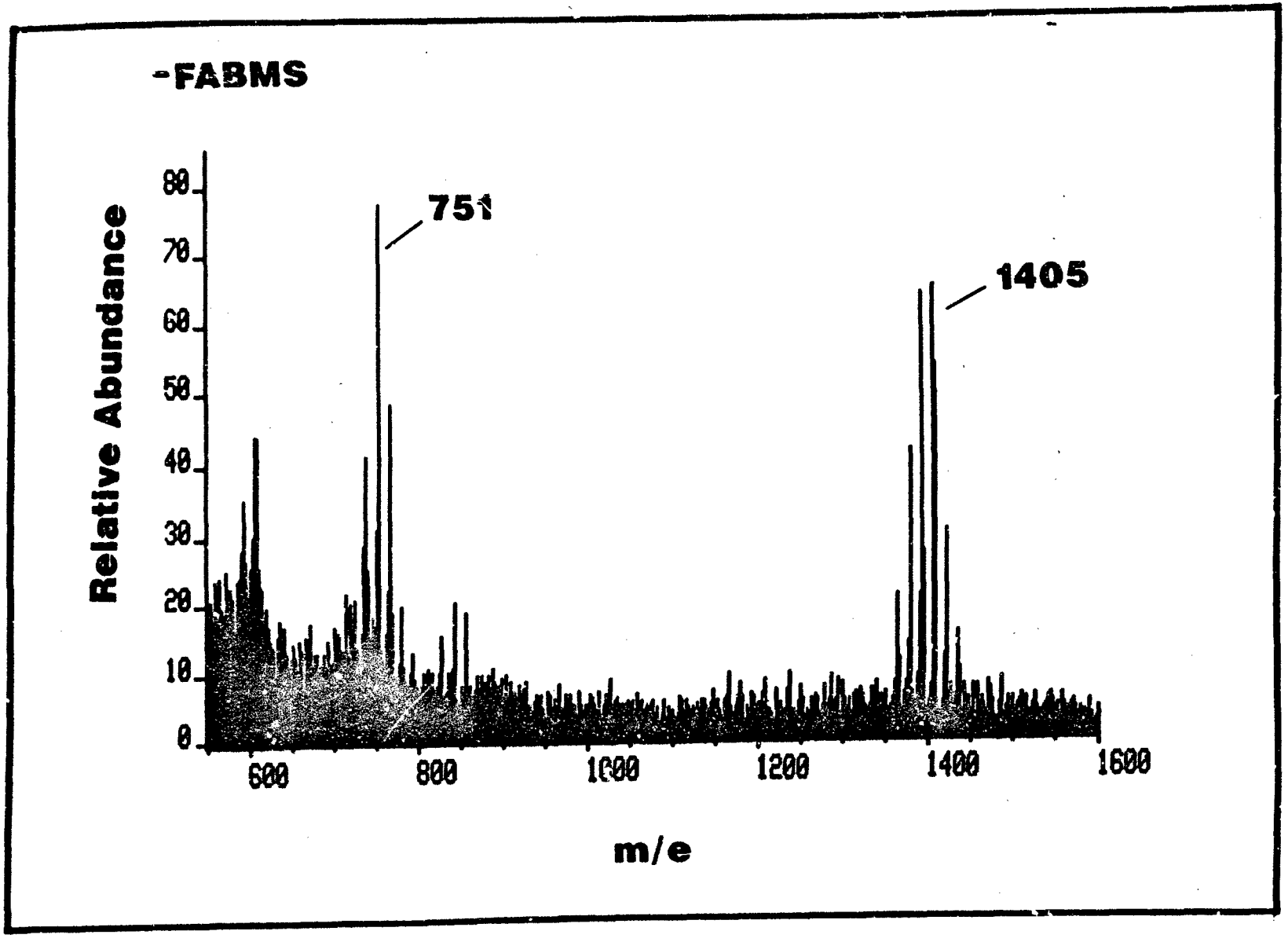
-FABMS
Relative Abundance
80
70
60
50
40
30
20
10
0
751
1405
600
800
1000
1200
1400
1600
m/e

Figure 9c

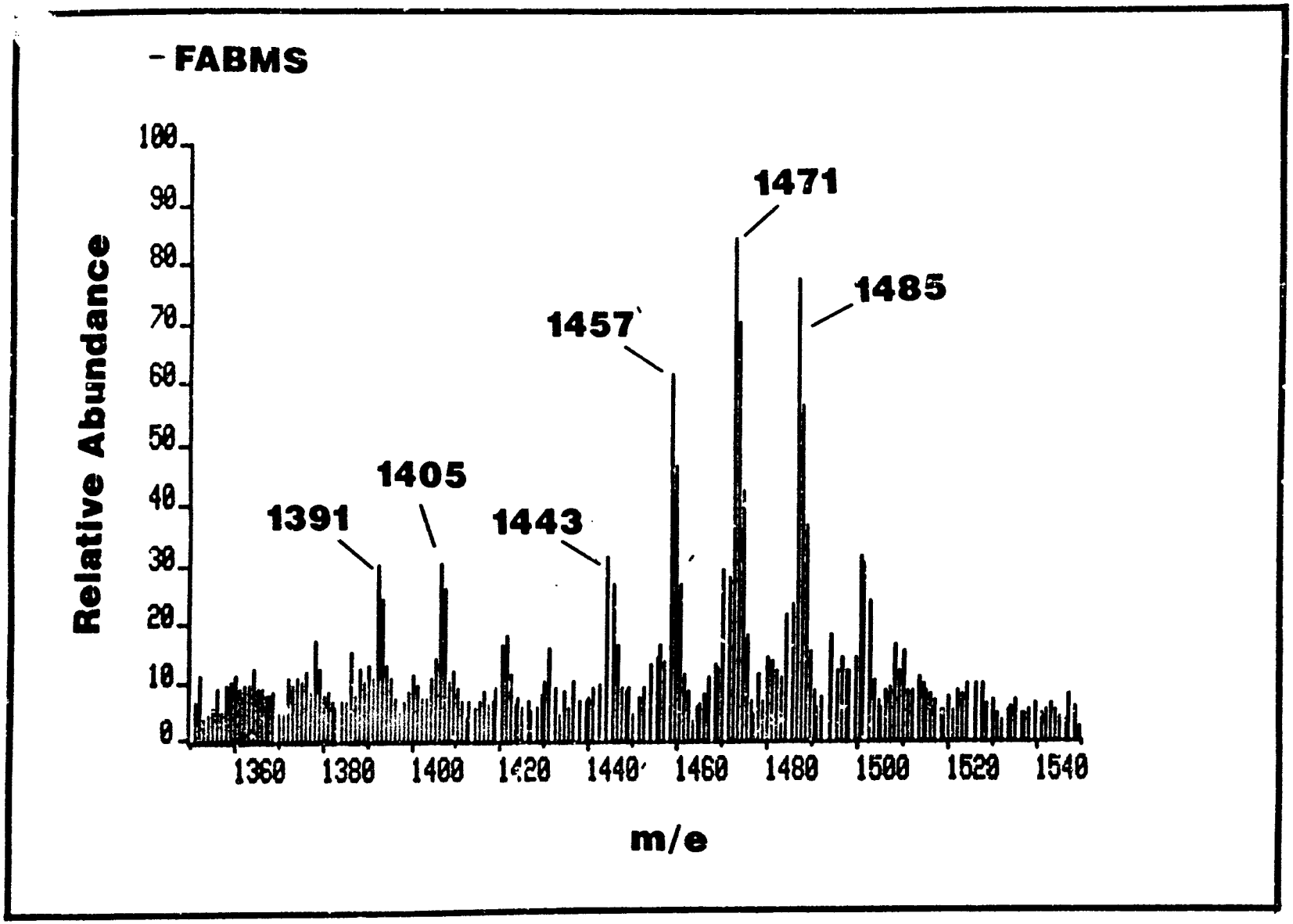
- FABMS
Relative Abundance
100
90
80
70
60
50
40
30
20
10
0
1391
1405
1443
1457
1471
1485
1360
1380
1400
1420
1440
1460
1480
1500
1520
1540
m/e

Figure 10

higher masses detected, there are significant differences observed between aqueous vs nonaqueous methanolysis. These results can now be understood as a consequence of the addition of one or more methyl groups, e.g., the masses are shifted by ±14 mass units. The shift from m/z 751 to 765 is quite apparent, and demonstrates the involvement of a hemiacetyl, carboxyl, or phosphate group, (Fig. 11). To define which of these groups are present the sample was reduced with $NaBH_4$. Analysis of these products indicated a 2 amu shift of the m/z 751 ion to 753, strongly suggesting a free reducing-end, (Fig. 12). Closer examination of this spectrum, however, shows incomplete reduction; note 2 amu lower satellite ions at m/z 751 and 765, but not for the sample lacking a phosphate group, m/z 671 and 685. This differential sensitivity to reduction may reflect isomeric structures as a consequence of methyl group location, as a methyl phosphate vs methyl glycoside. More interestingly, an associated pair of fragments incremented by 74 amu (m/z 825/839, see also Fig. 9a), also fails to shift upon reduction and is suggestive of an added glycerol moiety. This suggests that methanolysis yields three fragments; half of which are non-reducing methyl glycosides (Structure A, see below; also a small amount of a glycerol phosphate moiety, C), and the remaining half, a methyl phosphate residue that would provide a structure with a free reducing-end (A). These ion fragments can be accounted for by the following structures:

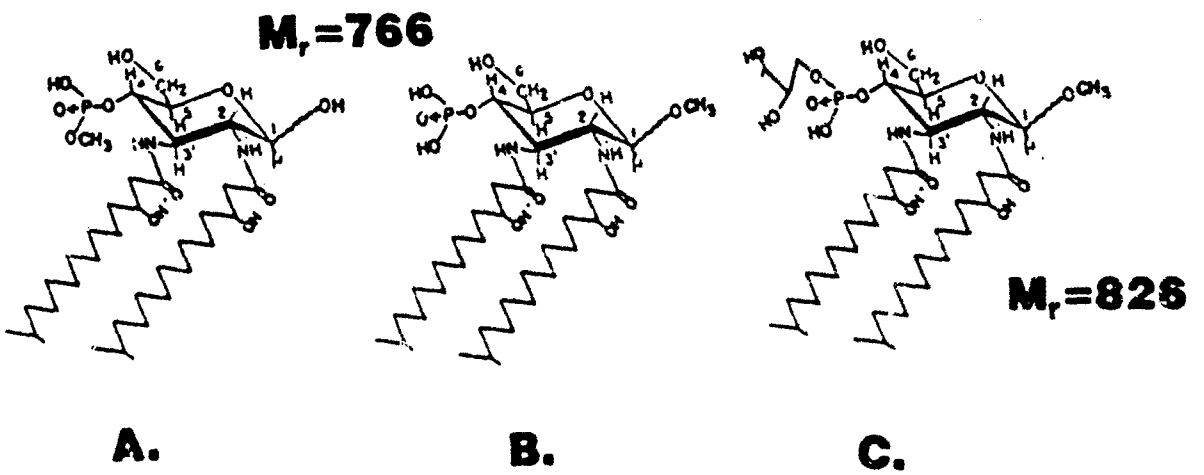

Further proof of these isomeric structures was approached by collision induced dissociation (CID) and peracetylation. In the former case ion focusing of m/z 765 and CID produced two daughter ion fragments in approximate equal abundance, (m/z 667 & 653), indicating an elimination of methyl phosphate and phosphate from the parent ion. These results corroborate the presence of the isomeric structures (A) and (B). Blocking the free hydroxyl groups and FABMS should also differentiate the isomeric m/z 765 structures by adding four (A) and three (B) groups. Peracetylation and negative ion FABMS provided the spectrum shown in Figure 13a. The mass shifts to m/z 891 and 933 represents the correct mass increments for the addition of three and four acetyl groups. The enhanced abundance for m/z 933 was not

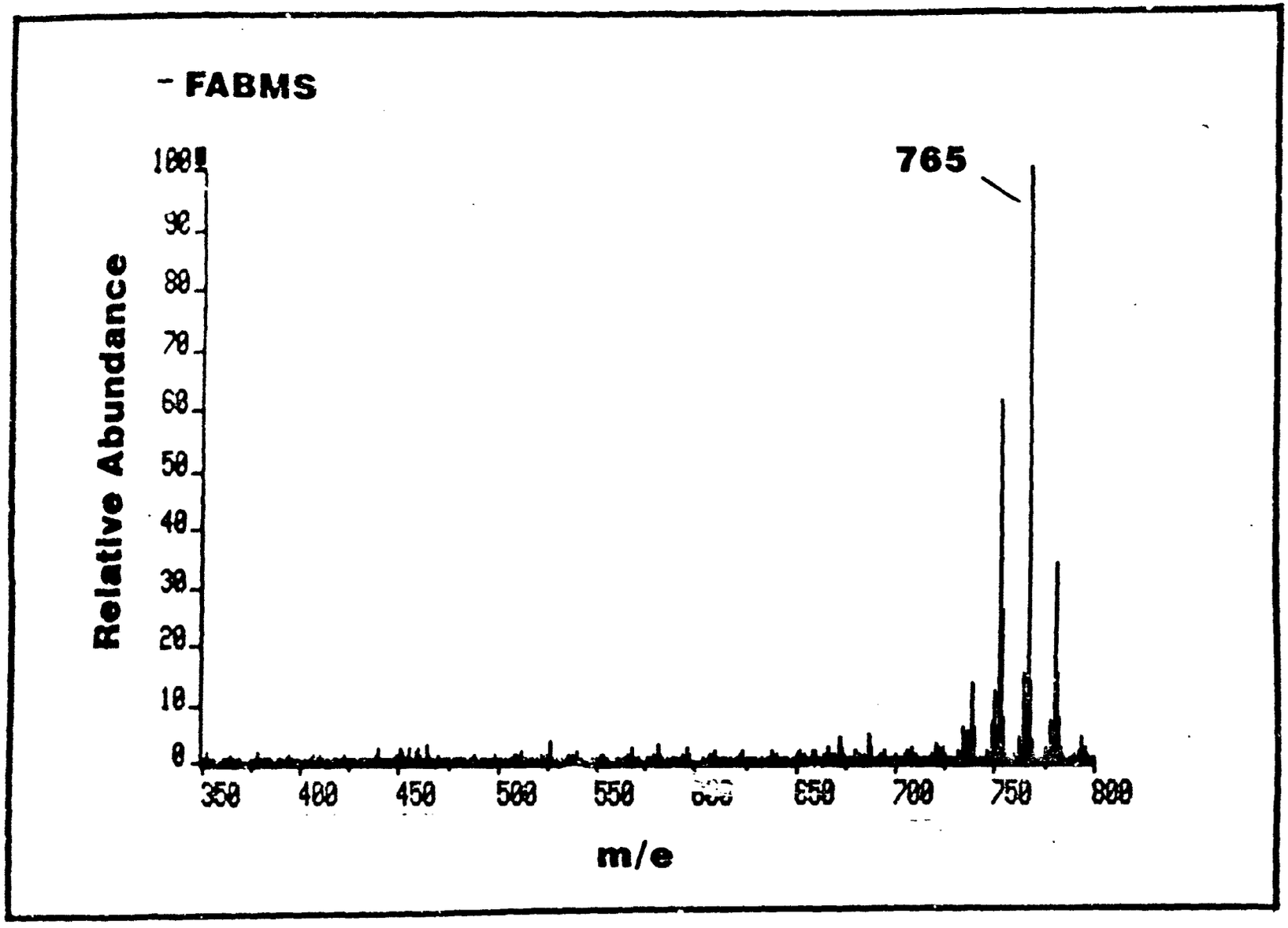
- FABMS
765
Relative Abundance
100
90
80
70
60
50
40
30
20
10
0
350
400
450
500
550
650
700
750
800
m/e

Figure 44

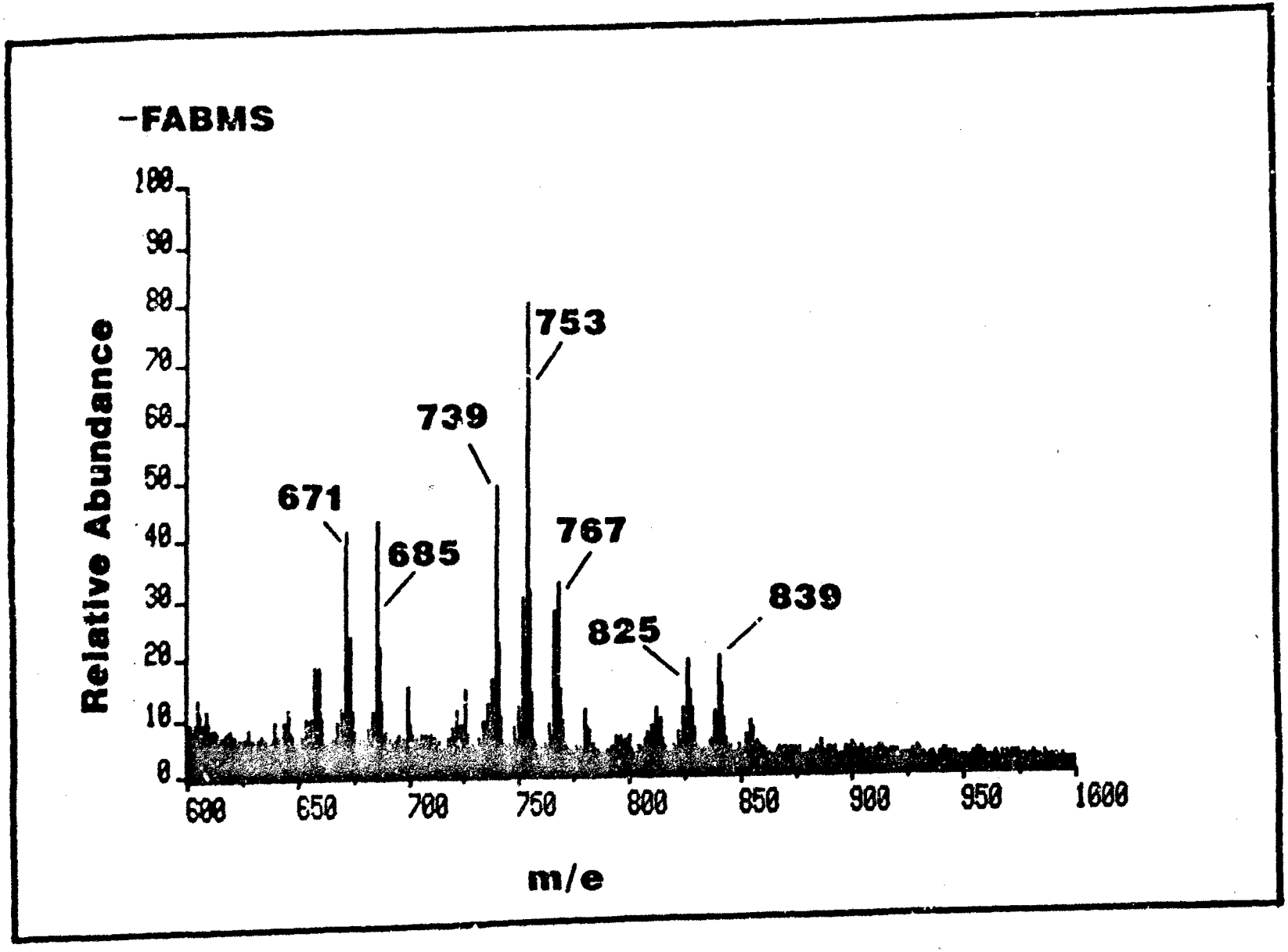
-FABMS
Relative Abundance
100
90
80
70
60
50
40
30
20
10
0
753
739
671
685
767
839
825
600
650
700
750
800
850
900
950
1000
m/e

Figure 12

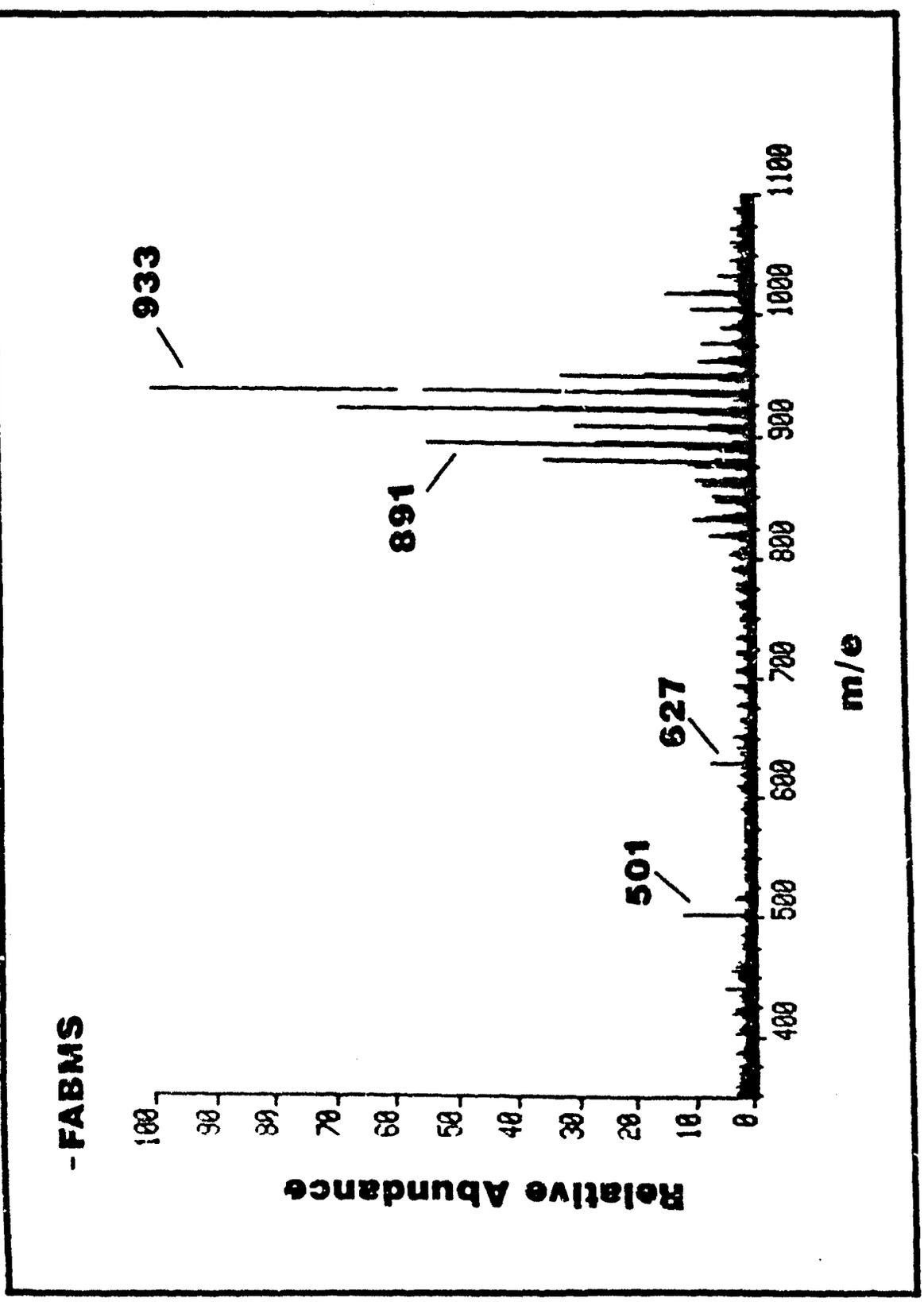
-FABMS
Relative Abundance
100
90
80
70
60
50
40
30
20
10
0
400
500
600
700
800
900
1000
1100
m/e
933
891
627
501

Figure 13a

anticipated but could represent incremental acylation at the amide hydrogens, (this partial reactivity was also observed when the heptaacyl monophosphoryl Lipid-A from Salmonella minnesota was peracetylated). The combination of CID, peracetylation, and reduction appears to support the two structures represented above.

To corroborate the number and type of carbohydrate-acyl linkages, the sample was investigated by base treatment. Two methods of basic hydrolysis were used, both known to induce complete de-O-acylate of carbohydrate samples and not effect N-acyl groups (25,29). Treatment of the peracetylated sample (Fig. 13a) with triethylamine in water, or ammonia in methanol and FABMS analysis of the products provided a spectrum identical with the starting material. This indicates that the added acetyl groups were O-linked and any other acyl groups are either amide- or ether-linked. Figure 13b shows the molecular ion region of the peracetylated methanolic hydrolysis product. The most abundant ions corresponds to the addition of seven acetyl groups, [(7 X 42) + 1406 = 1700] with a mass shift equal to two methylene residues caused by the incremental reactivity of the amide groups. This ion envelope does not show a split due to the difference in the number of acetyl groups, as was observed in Figure 13a for tri- and tetra-acetylated products. However, with such complexity it may be difficult to notice such detail. These results may be accommodated by the following structure:

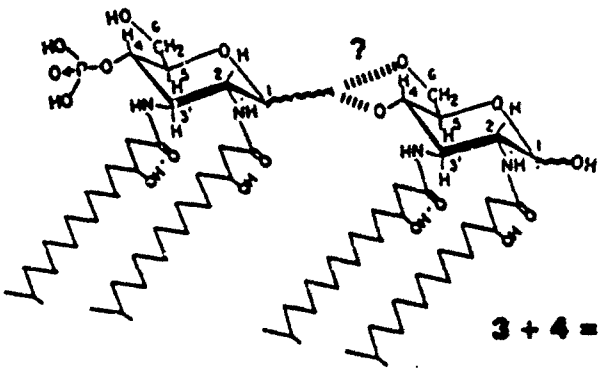

3 + 4 = 7 Free Hydroxyls

This work suggested the alkane heterogeneity may be linked through acyl-amide linkages; a consideration directly investigated by methanolysis with 3N HCl, (Fig. 14). These conditions are expected to induce quantitative methyl glycoside formation and cause partial acyl-amide degradation. As expected, the spectrum can be rationalized by considering de-N-acylation (monoacyl, m/z 433/457) and methyl esters of the released acyl groups (m/z 273/287). To further confirm the acyl-amide composition, the products m/z 657 and 737 were reduced and analyzed by +FABMS following treatment with diborane and deuterodiborane, procedures specific for amides (19,20):

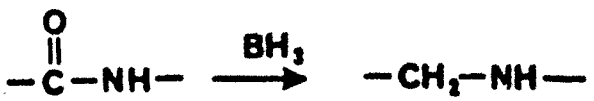

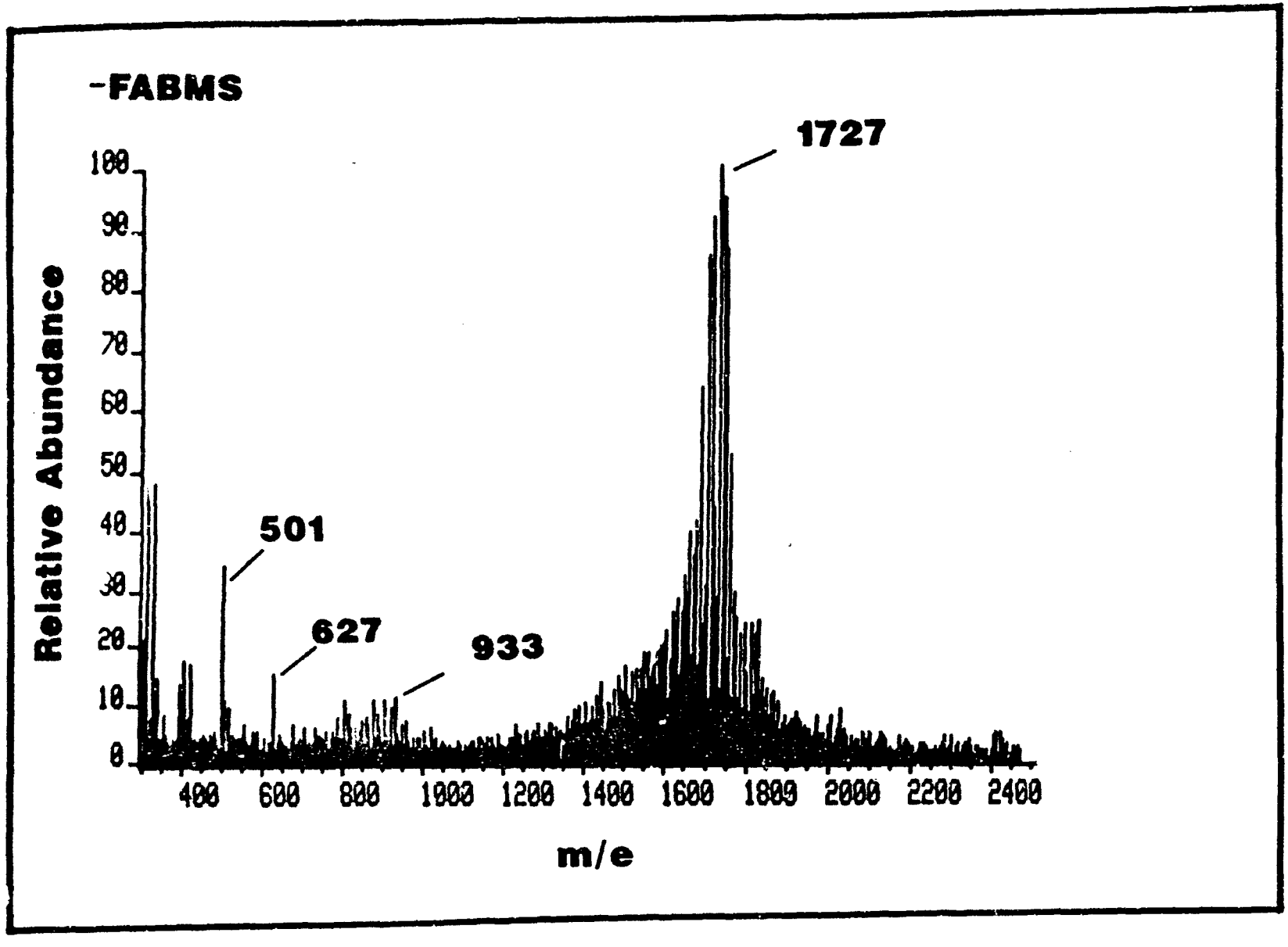
-FABMS
1727
501
627
933
Relative Abundance
100
90
80
70
60
50
40
30
20
10
0
400
600
800
1000
1200
1400
1600
1800
2000
2200
2400
m/e

Figure 13b

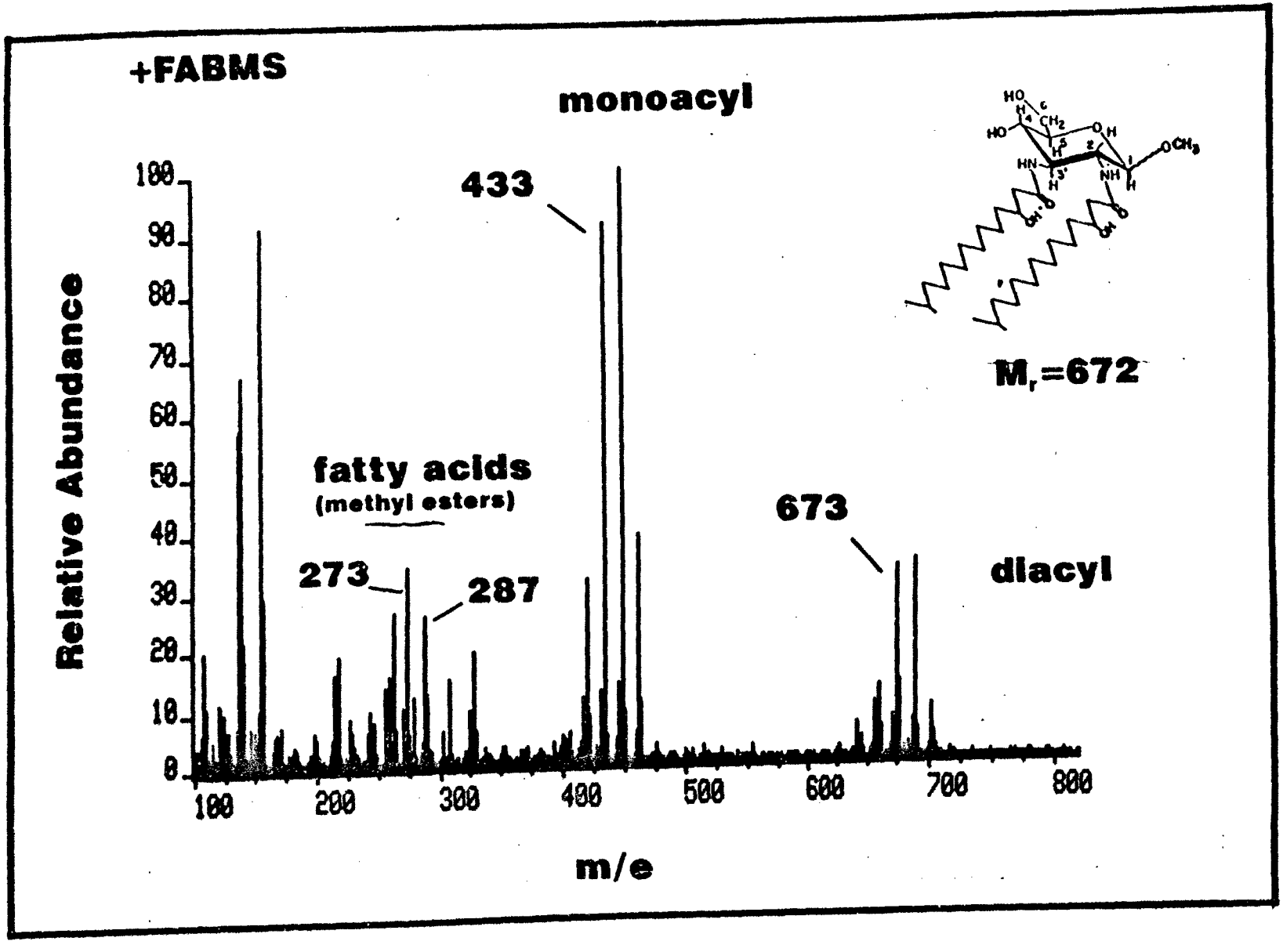
+FABMS
monoacyl
433
Relative Abundance
100
90
80
70
60
50
40
30
20
10
0
fatty acids
(methyl esters)
273
287
673
diacyl
100
200
300
400
500
600
700
800
m/e
M,=672

Figure 14

As shown above, the procedure reduces amides to amines decreasing a compounds mass by 14 amu for each amide residue, (this procedure also hydrates carbon-carbon double bonds incrementing the weight by 18 amu). This technique was applied to the methanolysis hydrolysis products to ascertain mass shifts associated with the diacyl glycose components, m/z 671/685, (Fig. 9a). The reduced material provided ions in the monomer area, m/z 645/659, (Fig. 15a), indicate a reduction in mass expected for the presence of two amide groups, (28 amu, incremented by 2 amu due to positive vs negative FABMS). Conformation of this amide reactivity was supported with deuterodiborane reduction, where the same products $(M+H)^+$ appeared four mass units higher, m/z 649/663, (Fig. 15b). The methylene envelope in the $(M + H)^+$ region introduces isobaric problems (28 amu shift) and deuterodiborane was necessary for confirmation. The assignments proved to be correct for the monomer, but, four deuterium atoms were not introduced into the phosphorylated monomer (m/z 739/735, Fig. 15a) indicating incomplete reduction. Control experiments with Lipid-A from Salmonella minnesota showed the same incomplete reduction. This Lipid-A contains two amide groups, and only one reduced; thus, it would seem as though a proximal phosphate group on the terminal amino sugar somehow interferes with this reaction.

Fatty acids are not released under de-O-acylation conditions suggesting them to be either ether or amide linked. Reduction with BH_3 supports the latter possibility and the mass shift indicates two such groups. Ether linkages has been observed in archaebacterial membranes (12), but this data indicates acyl linkages to amide groups of a diamino hexose, as observed in other LPS's (27,31). Furthermore, the molecular weight of this subunit is in agreement with what would be expected given the amount and types of fatty acids previously described (32,33).

The above data has indicated two amide groups, linked with a homologous fatty acids series. Satellite clusters 80 amu above and below other prominent ion clusters suggest the presence of phosphate. Collision of the isobaric components, m/z 765, and daughter ion analysis have shown losses of 98 and 112 amu, a mass equal to phosphate and methyl phosphate, respectively. To obtain more direct evidence, samples were treated with diazomethane to methylate phosphoryl groups and the products analyzed by FABMS, (Fig. 16). Two clusters are observed, surrounding the ions m/z 687 and 795; the former cluster appears unchanged and appears at the expected mass for molecules not containing phosphate, (cf., m/z 673/685, Fig. 14). The latter group of ions shifted upwards by 28 amu, (cf., unmethylated, Fig. 11), expected for a dimethylphosphoryl ester. When the most abundant ion in this envelope, m/z 795, was mass selected and fragmented by CID an abundant fragment (daughter ion) was detected at m/z 669, Fig. 17. This can be accounted for by considering a dimethylphosphate elimination.

Two amide groups, an aliphatic fatty acid series, and a phosphate group are components of the monomer structure. The location of the phosphate group was investigated by reduction, periodate oxidation, aldehyde trapping with methoxime and acetylation, (see Page 8, Section B. a). A methanolic hydrolysis of Lipid-A was carried out to obtain higher yields of the monomer (M_r = 752) (Fig. 9a). This sample was reduced to the alditol with $NaBH_4$ and the product periodate oxidized, methoximated, and acetylated. Analysis by -FABMS provided

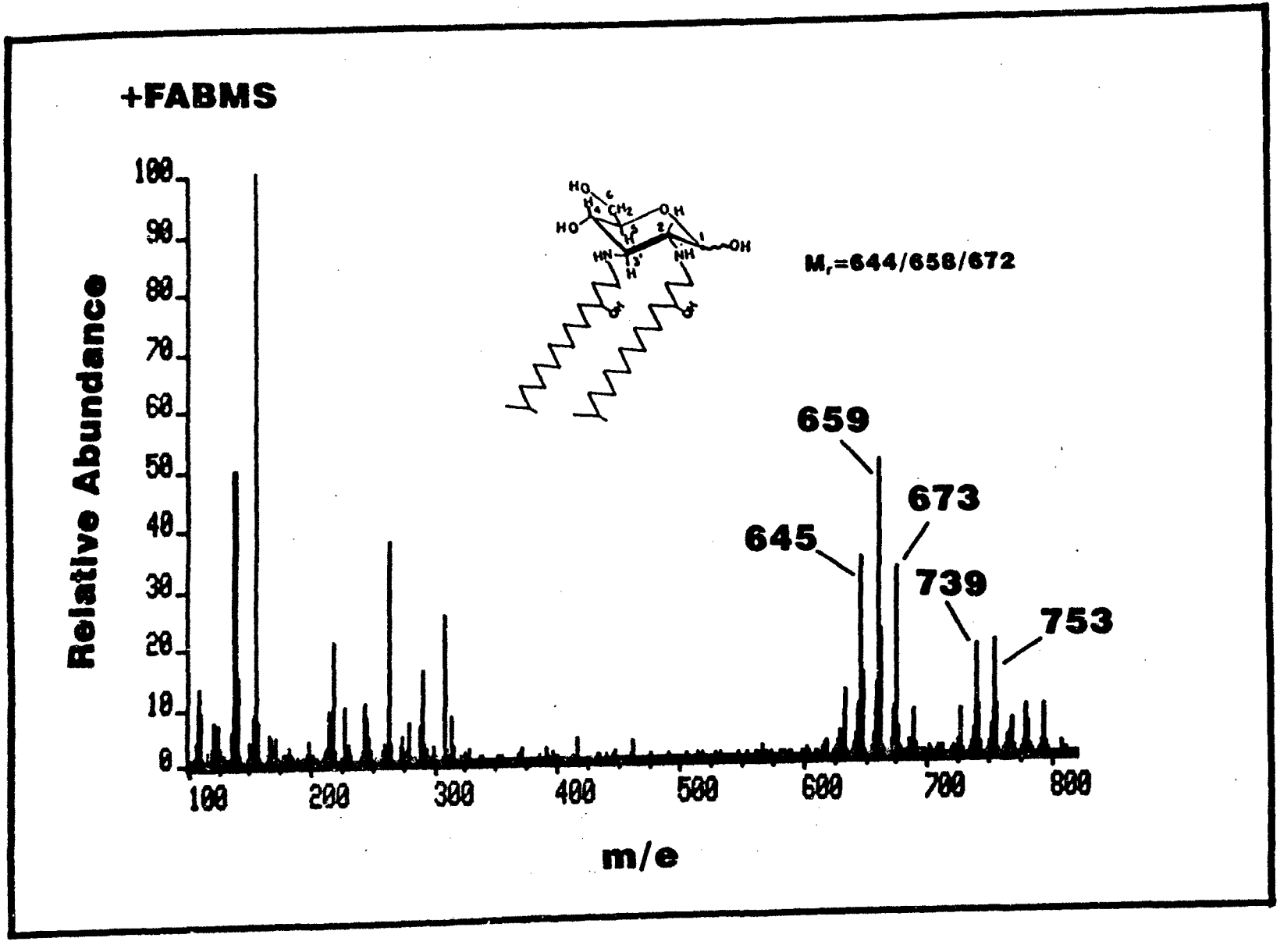
+FABMS
Relative Abundance
100
90
80
70
60
50
40
30
20
10
0
100
200
300
400
500
600
700
800
m/e
M,=644/658/672
659
673
645
739
753

Figure 15a

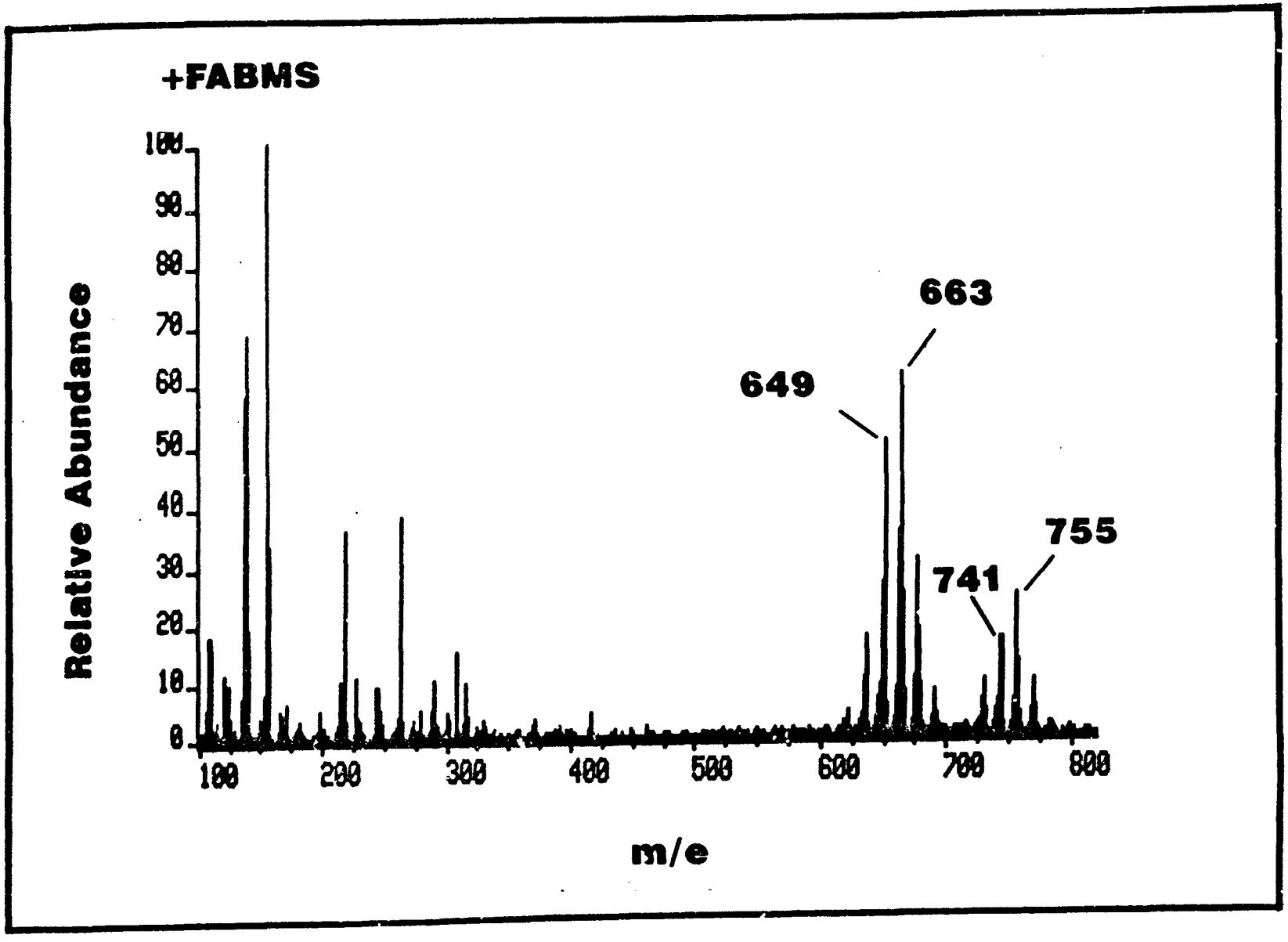
+FABMS
Relative Abundance
100
90
80
70
60
50
40
30
20
10
0
100
200
300
400
500
600
700
800
m/e
663
649
755
741

Figure 15b

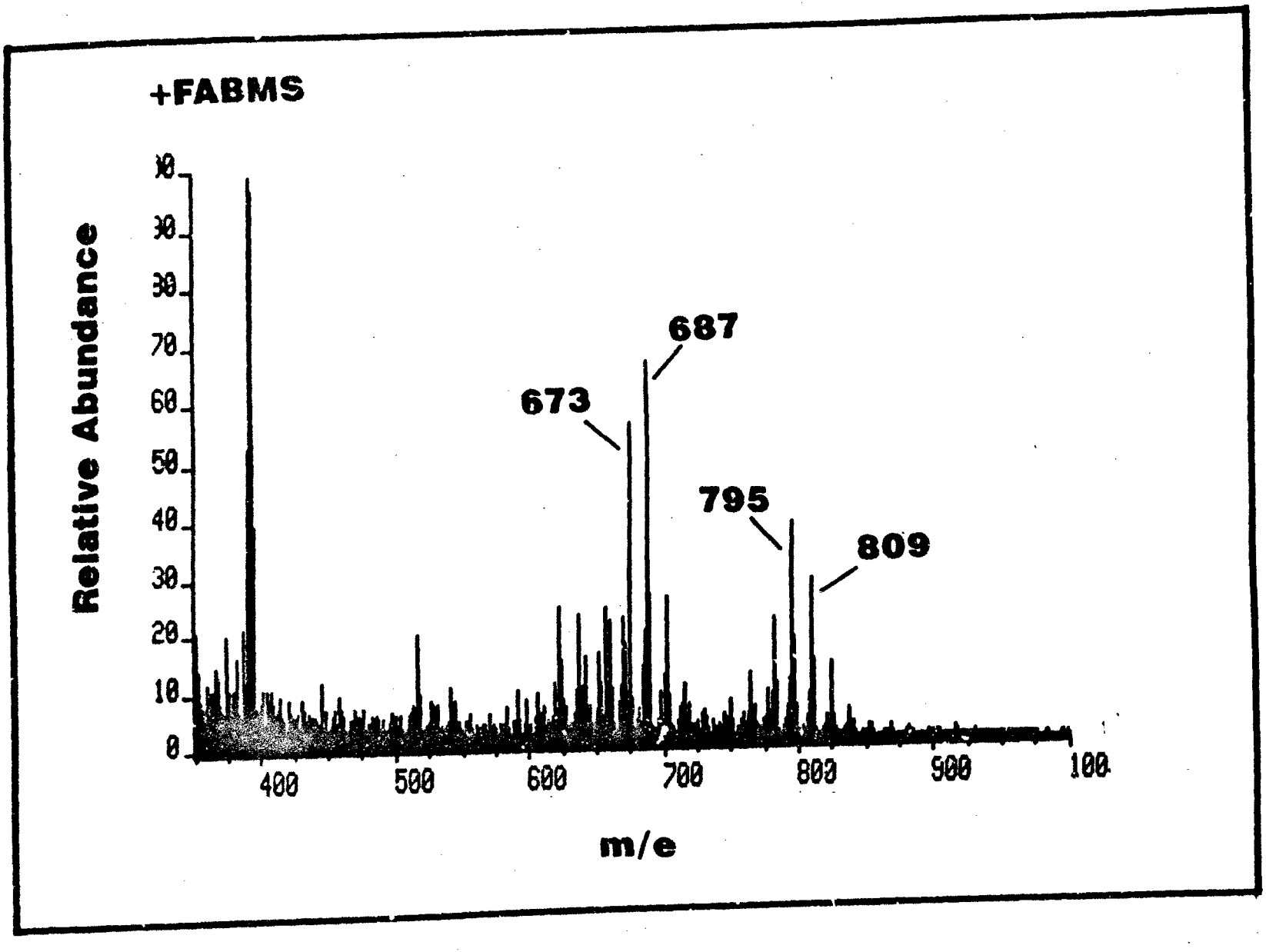
+FABMS
Relative Abundance
100
90
80
70
60
50
40
30
20
10
0
400
500
600
700
800
900
1000
m/e
687
673
795
809

Figure 16

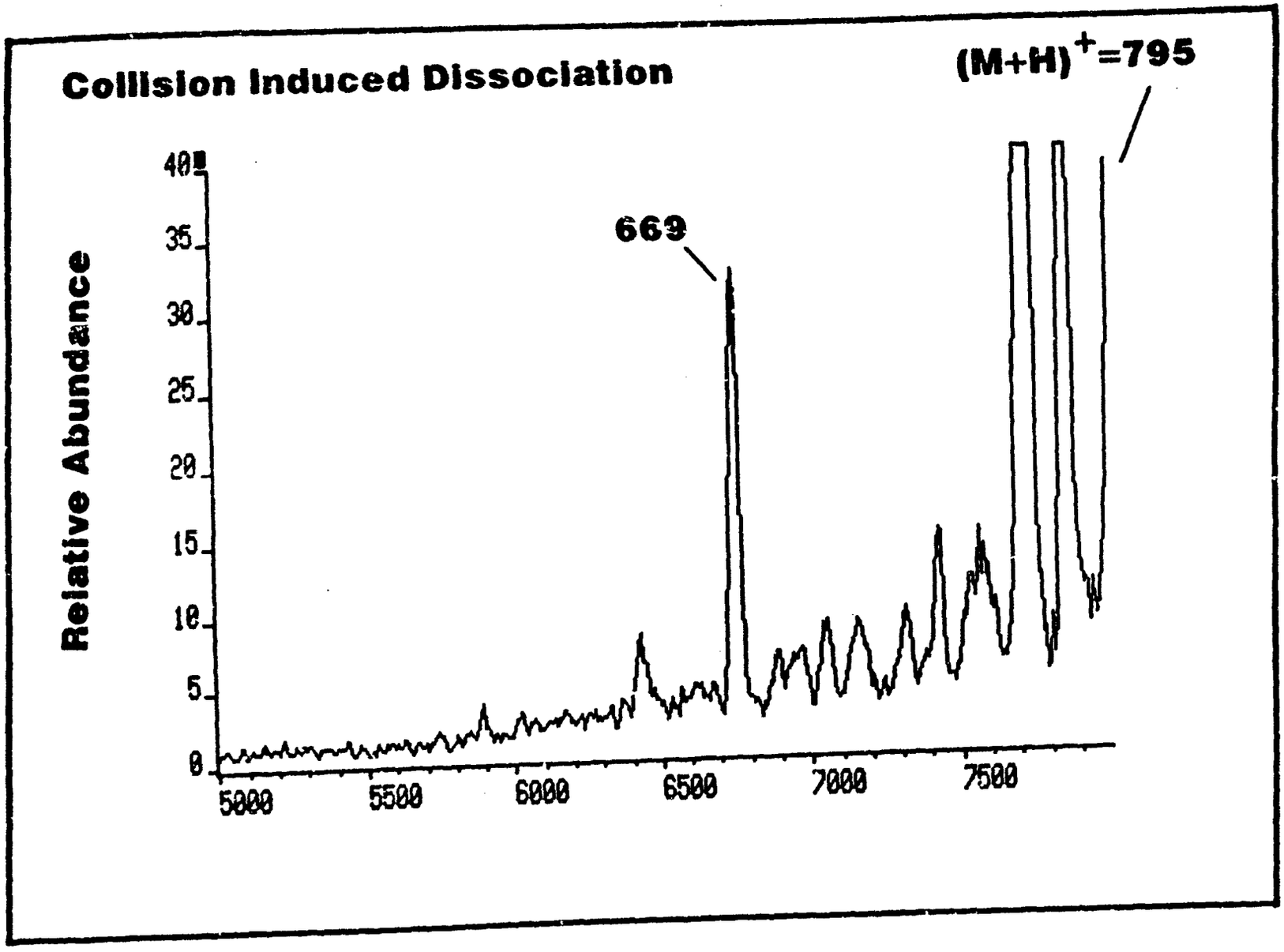
Collision Induced Dissociation
(M+H)+=795
669
Relative Abundance
40
35
30
25
20
15
10
5
0
5000
5500
6000
6500
7000
7500

Figure 17

an ion at m/z 875 (Fig. 18) which can be accounted for by considering periodate cleavage of a 5,6-diol, placing the phosphate group at position 4, (Scheme II, A = 6-O-, B = 4-O-Phosphate).

The 4-O-phosphoryl-diacyl-diamide monomer was suspected to be 2,3-diamino-2,3-dideoxy glucose, a component previously identified in other Lipid-A samples (27). To check this possibility, a Lipid-A fraction was extensively washed and hydrolyzed under very harsh conditions (6 N HCl at 100 °C for 18 hrs) to remove all amide-linked fatty acids. The released fatty acids were extracted and the aqueous fraction dried, N-acetylated and O-silylated and compared with a commercially available sample. The Coxiella burnetii derived sample was identical to that of a standard 2,3-diamino-2,3-dideoxy-D-glucose sample, as determined by gas chromatography after derivatization.

This data confirms the amino sugar present in Coxiella burnetii Lipid-A to be a 2,3-dideoxy-2,3-diamino-D-glucose with each amino group acylated to provide a monomer molecular weight of 672 daltons. These acyl-amide residues impart an envelope of molecular ions differing by 14 amu characteristic of the aliphatic methyl ester determined earlier (33). Of the two phosphate groups, one is located at position C'-4 on the non-reducing amino sugar monomer, and the second is located on the reducing amino sugar at either position C-4 or C-6. Dimer linkage analysis is currently undergoing studies with model compounds according to the diagram presented in Scheme III. Placement of this linkage would establish, by default, the position of this second phosphate group. Consistent with other Gram-negative species, this O-antigen membrane anchor appears to be an amino sugar dimer providing a molecular weight equal to 1486 daltons. A summary of these results are presented below:

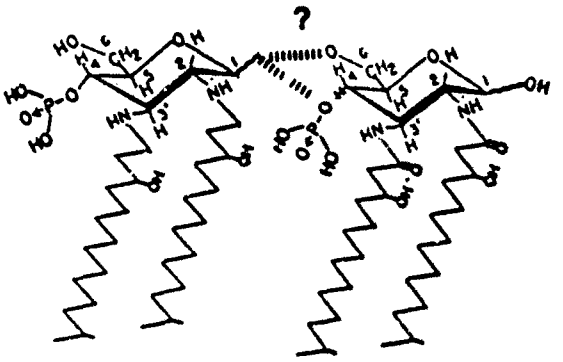

An interesting finding, in the unraveling of this LPS structure, is the apparent alkane heterogeneity that exists in Lipid-A. Fatty acid methyl ester analysis of Lipid-A preparations isolated earlier suggest this heterogeneity originates with these acyl groups, but since these are total compositional analysis, site specific conjugation remains to be determined. Moreover, since successful attempts at extraction and isolation have always involved methanol, a technical question must be considered whether this apparent alkane heterogeneity (14 amu intervals) may in fact be due to partial ester formation on phosphates or glycoside formation on hemiacetyls (also providing 14 amu intervals). To address these questions we have underway two expensive experiments involving stable isotope. The

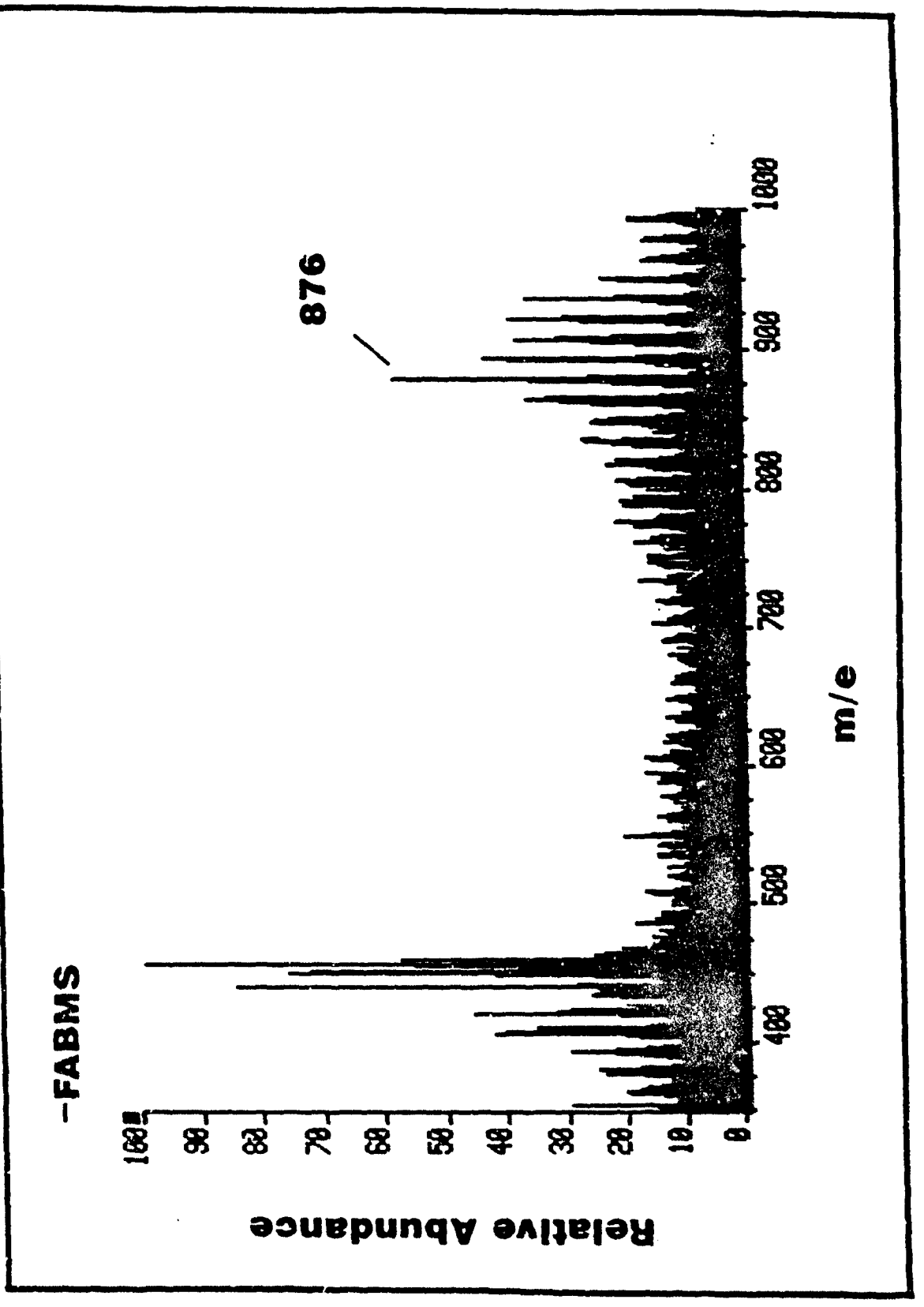
-FABMS
Relative Abundance
100
90
80
70
60
50
40
30
20
10
0
400
500
600
700
800
900
1000
m/e
876

Figure 18

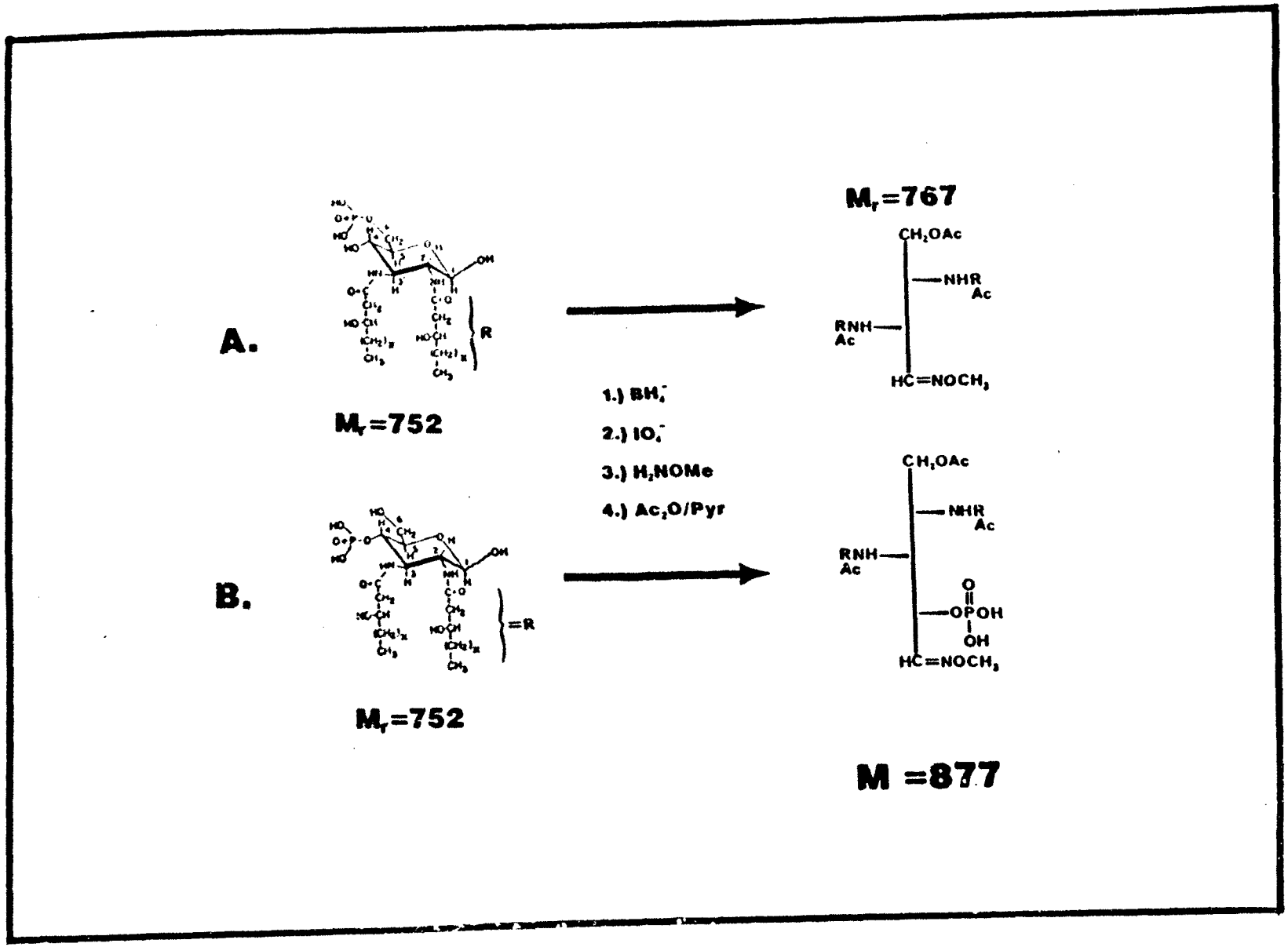
A.
M$_r$=752
R
1.) BH_4^-
2.) IO_4^-
3.) H_2NOMe
4.) Ac_2O/Pyr
M$_r$=767
CH$_2$OAc
NHR
Ac
RNH
Ac
HC=NOCH$_3$
B.
M$_r$=752
=R
CH$_2$OAc
NHR
Ac
RNH
Ac
O
OPOH
OH
HC=NOCH$_3$
M =877

Scheme II

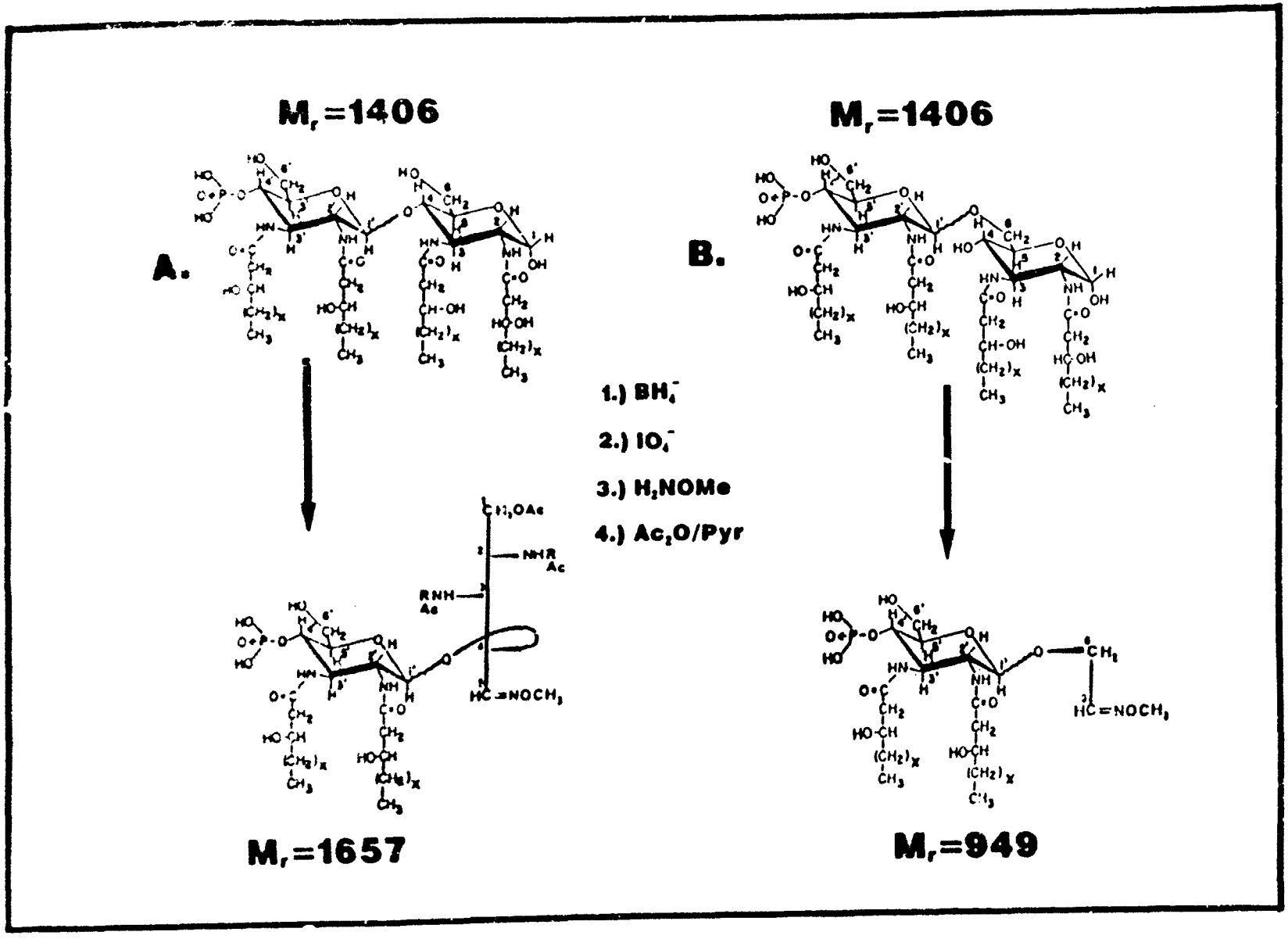

Scheme III

Acyl-amide Microheterogeneity

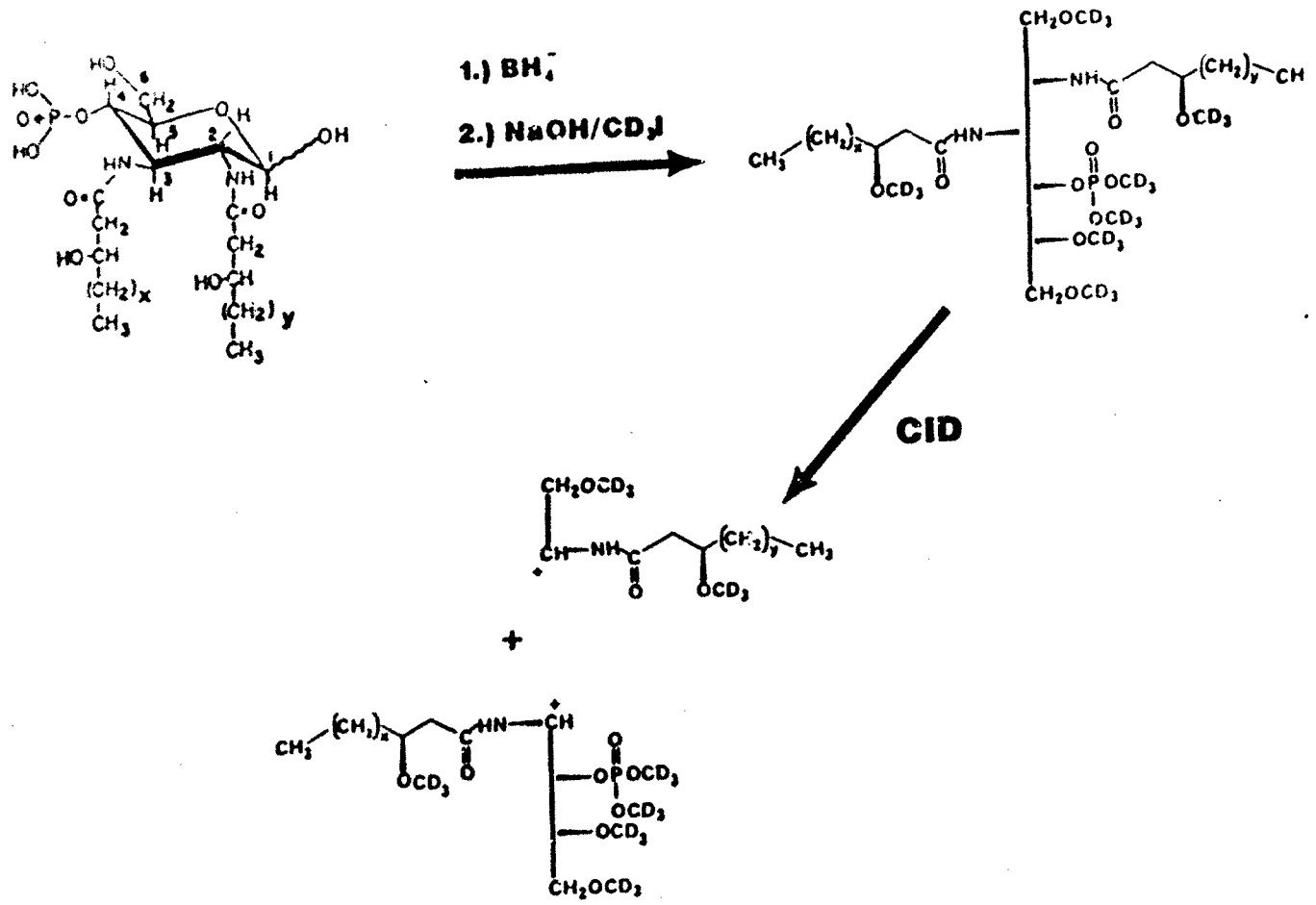

Scheme IV

first in methanolysis hydrolysis in the presence of CD_3OD and check alkane heterogeneity; the second experiment will involve reduction and perdeuteriomethylation of the monomer, m/z 751.5 (Fig. 9b). Collision should provide daughter ion fragments between the labile C_2-C_3 bond splitting the acyl-amide groups. Multiple or single daughter ion fragments would answer the problem of site-specific alkane heterogeneity, (Scheme IV).

Three strains from phase I, phase II, and the intermediate phase (strains 9MIC7, 9MIIC4, and RSA514, respectively) were each subjected to both methanolysis and methanolic hydrolysis, examined by negative FABMS, and all gave similar spectra (Figs. 9 and 10). These results seem to suggest that the differences in the virulent and avirulent phases are due to the oligosaccharide portion of the LPS and not in the Lipid-A moiety.

REFERENCES SENSITIVITY

1.) Hase, S., Ikenaka, T., and Matsushima, Y. (1978). Biochem. Biophys. Res. Commun. 85, 257-263.
2.) Hase, S., Natsuka, S., Hisashi O., and Ikenaka, T. (1987). Anal. Bochem., 167:321-326.
3.) Reinhold, V.N., Coles, Eric., and Carr, S.A. (1983). J. Carbohydr. Chem. 2:1-18.
4.) Wang, W.T., LeDonne, Jr., N.C., Ackerman, B., and Sweeley, C.C. (1984). Anal. Biochem., 141:366-381.
5.) Her, G.-R., Santikarn, S., Reirhold, V.N., and Williams, J.C. (1987). J. Carbohydr. Chem. 6:129-139.
6.) Hardy, M.R. and Townsend, R.R. (1988). Proc. Nat. Acad. Sci. (USA), 85:3289-3293.
7.) Hardy, M.R. and Townsend, R.R. (1989). Carbohydr. Res. 188:1-7.
8.) Webb, J.W., Jiang, K., Gillece-Castro, B.L., Tarentino, A.L., Plummer, T.H., Byrd, J.C., Fisher S.J., and Burlingame, A.L. (1988). Anal. Biochem. 145:337-349.
9.) Kawahara, F.K. (1968). Anal. Chem. 10:1009-1010.
10.) Kawahara, F.K. (1968). Anal. Chem. 10:2073-2074.
11.) Wickramasinghe, J.A.F., Morozowich, W., Hamlin, W.E., Shaw, S.R. J. Pharm. Sci., 62:1428-1431(1973).
12.) Min, B., and Pao, J., Garland, W., deSilva, J., and M. Parsonnet. (1980). J. Chrom. 183:411-419.
13.) I. Blair, S. Barrow, K. Waddell, P. Lewis and C. Dollery. (1983). Prostaglandins, 23:579-589.
14.) Waddell, K., Blair, I., and Wellby, J. (1983). Biomed. Mass Spec. 10:83-88.
15.) Strife, R., and Murphy, R. Jour. Chrom., 305:3-12 (1984)
16.) Angel A-S, Lindh F, Nilsson B. Carbohydr Res, 168:15-31 (1987).
17.) Reinhold VN. (1989) Proc. of the 37th ASMS Conf on Mass Spect. and Allied Topics, May 21-26, Miami, FL. p.1476.
18.) Lipid-A paper
19.) Vath JE, Zollinger M. Biemann K. (1988) Fresenius Z Anal Chem 331, 248-252.
20.) Vath JE, Biemann K. (1988). Proc. of the 36th ASMS Conf on Mass Spect. and Allied Topics, June 5-10, 1988, San Francisco, CA, p.167.
21.) Sonesson A, Bryn K, Jantzen E, Larsson L. (1989) J Chromatogr, 487, 1-7.
22.) Bryn K, Jantzen E. (1982) J Chromatogr 240, 405.
23.) Ciucanu I, Kerek F. (1984) Carbohydr Res, 131, 209-217.
24.) Qureshi N, Mascagni P, Ribi E, Takayama K. Monophosphoryl Lipid-A obtained from lipopolysaccharides of Salmonella minnesota R595. J Biol Chem, 260:5271-5278(1985).
25.) Qureshi N, Takayama K, Ribi E. Purification and structural determination of nontoxic lipid A obtained from the lipopolysaccharide of Salmonella typhimurium. J Biol Chem, 257:11808-11815(1982).
26.) Rietschel ET, Hase S, King MT, Redmond J, Lehmann V. (1977) Microbiology (Schlessinger D. ed) pp 262-268, American Society of Microbiology, Washington DC.
27.) Galanos C, Luderitz O, Rietshel ET, Westphal O. (1977) Int Rev Biochem, 14:280-288.
28.) Qureshi N, Takayama K, Heller D, Fenselau C. J Biol Chem, 258:12947-12951(1983).

29.) Reinhold VN. Methods in Enzymology, 25:244-249(1972).
30.) DeRosa M, Gambacorta A, Gliozzi A. (1986) Microbiol Rev, 50, 70-80.
31.) Mayer H, Weckesser J. In: Handbook of Endotoxin, Vol. 1: Chemistry of Endotoxin, Ed., E.T. Rietschel, Elsevier Science Publishers, pp. 232-234, 1984.
32.) Wollenweber H-W, Schramek S, Moll H, Rietschel ET. (1985) Arch Microbiol, 142, 6-11.
33.) Annual and Final Report Submitted to USAMRIID 30 November 1987, page 28. Her GR and Reinhold VN.

FIGURE LEGENDS

Figure 1a: UV Absorbance Scans of PFBAB (———), and PFBAB-maltoheptaose (— — —). Absorption maxima at 292 and 296 nm, respectively.

Figure 1a: Fluorescence Scans of PFBAB-fucose. Excitation wavelength = 296 nm. Scan rate = 1 sce/nm. A = 1.2μm; B = 24.0nm; C = 6.0nm; D = 12.0nm; E = solvent blank.

Figure 2: Supercritical fluid chromatography of PFBAB labeled maltodextrin sample prepared as the acetate derivative. Cyanopropyl SFC column using CO_2 as the mobile phase.

Figure 3: Sensitivity study using PFBAB labeled fucose. Product ion (m/z 408) loss of PFB group. Mass spectrum taken at dilution of 55 femtomoles. Insert showing mass chromatograph at m/z 408 and expanded spectral scan.

Figure 4: SFC-MS of PFBAB-labeled highly branched glycan obtained from plant lectin by endoglycosidase treatment. Foreground, total ion plot with mass chromatograms (ion plots) offset to the right for selected components in the complex mixture. M = mannose, G = glucosamine. Note resolution of branched isomeric doublet at M_7G.

Figure 5: Positive ion fast atom bombardment mass spectrum of highly branched Man_6GN sample labeled with pyridinylamine. Previous to FABMS analysis sample was prepared for sequence, linkage and branching studies by periodate oxidized, methoximation, and acetate derivatization.

Figure 6: SFC negative ion chemical ionization mass spectrum (SFC-NCI-MS) of PFBAB labeled Man_8GN isolated from plant lectin prepared for linkage, sequence, and branching studies by periodate oxidation and derivatization.

Figure 7: Expected results of combined SFC-NCI-MS-CID-MS analysis of complex branched glycan. Sample prepared as nitrile derivative. CID provides monomer mass intervals for sequence, periodate oxidation yields linkage and branching, and $(M-H)^-$ ion yields M_r and supporting linkage and branching information.

Figure 8: SFC of Lipid-A obtained from Salmonella minnesota Re595 sample prepared by acetylation. Cyanopropyl column with FID detection. Structure and peak correlation by isolated TLC fractions only; SFC-MS studies expected to be completed soon.

Figure 9a: Aqueous methanol hydrolysis of CB514 organic phase analyzed by negative ion FABMS.

Figure 9b: Aqueous methanol hydrolysis (1.5N HCl) of CB9MIC7 organic phase analyzed by negative ion FABMS.

Figure 9c: Aqueous methanol hydrolysis (0.15N HCl) of CB9MIC7 organic phase analyzed by negative ion FABMS. Dimer area in high conc.

Figure 10: Methanolic hydrolysis (1% HoAc) of CB9MIC7 organic phase analyzed by negative ion FABMS. Added phosphoryl group.

Figure 11: Negative ion FABMS of monomer prepared in 3N HCl methanol. Two component isomeric mixture by CID, reduction, and acetylation.

Figure 12: Negative ion FABMS of monomer and monomer phosphate prepared by reduction with $NaBH_4$.

Figure 13a: Negative ion FABMS of monomer following peracetylation. Determination of free hydroxyl groups.

Figure 13b: Negative ion FABMS of dimer phosphate prepared by peracetylation; Determination of free hydroxyl grooups.

Figure 14: Positive ion FABMS of monomer following 3N HCl hydrolysis. Acyl-amide methanolysis to produce monoacyl monomer and fatty acid methyl esters.

Figure 15a: Positive ion FABMS of monomer by BH_3 gas phase reduction of amides to corresponding amines.

Figure 15b: Positive ion FABMS of monomer by BD_3 gas phase reduction of amides to corresponding amines.

Figure 16: Positive ion FABMS of monomer and monomer phosphate following diazomethylation for phosphate methylation analysis.

Figure 17: Collision induced dissociation spectrum of monomer phosphate indicating methyl phosphate elimination.

Figure 18: Negative ion FABMS of monomer phosphate following reduction, periodate oxidation, aldehyde trapping, and acetylation.